ACS Sustainable Chemistry & Engineering

Perspective

Cite This: ACS Sustainable Chem. Eng. 2019, 7, 49−69

pubs.acs.org/journal/ascecg

Crystal Engineering of Metal−Organic Framework Thin Films for Gas Separations

Deepu J. Babu,[†] Guangwei He,[†] Luis Francisco Villalobos,[†] and Kumar Varoon Agrawal*

Laboratory of Advanced Separations (LAS), École Polytechnique Fédérale de Lausanne (EPFL), EPFL Valais Wallis, Rue de l'Industrie 17, Sion 1950, Switzerland

ABSTRACT: Metal−organic frameworks or MOFs have witnessed a phenomenal rise owing to a highly tunable synthetic chemistry allowing flexibility in the selection of its constituents, namely metal nodes and linkers. Combined with their superior adsorption and diffusion properties, MOFs have become one of the most promising nanoporous materials for the fabrication of high-performance membranes. Polycrystalline MOF membranes have yielded one of the best gas separation performances, and are expected to replace or partially substitute thermally driven separation processes. In this respect, we present our perspective on the crystal engineering of MOF films that offers control over nucleation and growth of MOFs, film morphology, lattice defects, and therefore the separation performance of the resulting MOF films.

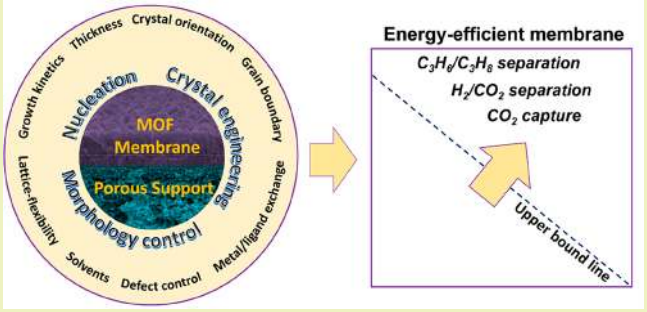

KEYWORDS: *Polycrystalline membrane, Metal−organic frameworks, ZIF, Gas separation, Defects, Lattice flexibility*

INTRODUCTION

Membrane-based separations are going to play a major role in improving the energy-efficiency of molecular and ionic separations that currently accounts for 40−70% of the energy footprint as well as the capital cost in the chemical plants.[1] Membrane processes, by design, are simple, clean, and environmental-friendly, and are amenable for process-intensification. The current generation of molecular-separation membranes is based on dense polymeric films attributing to the fact that the polymers can be conveniently casted into a thin film, and as a result, can be easily scaled-up. However, the application of the polymer-based membranes is severely restricted by their chemical, thermal and mechanical stability, and an intrinsic performance trade-off (Robeson upper bound).[2,3] The performance of polymeric membranes can be improved by engineering its free-volume (e.g., thermally reduced polymers[4] and polymers with intrinsic microporosity[5]) or by developing mixed-matrix membrane approaches, to obtain high rigidity as well as high porosity,[6] albeit disrupting the processability and cost advantages of polymers. Yet, more development is needed to meet the performance target (a combination of selectivity and permeance where permeance, defined by permeability normalized by thickness, is the realistic measure of gas flux from a given membrane) for several crucial separation applications such as carbon capture, hydrogen recovery, hydrocarbon splitting, O_2/N_2 separation, etc.

An ideal membrane material should (i) possess a high porosity to maximize permeability, and a pore-structure to differentiate molecules based on their adsorption and diffusion properties; (ii) be conducive to surface and pore-modifications to further tune the adsorption and diffusion selectivities; (iii) be easy to synthesize and to engineer into a thin film morphology, preferably with a thickness of 1−100 nm; and (iv) be stable at the operating conditions, preferably at the high pressure and temperature conditions. In this respect, metal−organic frameworks (MOFs) have emerged as the most promising nanoporous material to either substitute or to supplement the polymeric membranes, evident by the increasing number of publications of MOF with respect to other class of materials (Figure 1). MOFs are hybrid inorganic/organic coordination compounds made by joining organic linkers with metal nodes, leading to a crystalline framework with a permanent microporosity.[7] The flexibility in the selection of metal and organic building blocks, the underlying reticular chemistry, and a relatively rapid crystallization kinetics have allowed the synthesis of thousands of MOF structures for a wide range of applications including gas storage,[8] separations,[9,10] catalysis,[11,12] fuel cells,[13] supercapacitors,[14] electronic and optoelectronic devices,[15] dielectric layer,[16] etc. MOFs with a wide range of pore-topology, pore-window, cages, functionality, and chemical composition have been synthesized, while a much larger set has been theoretically predicted.[17,18] Several of these structures are promising for gas separation, the topic of this review.

This review uniquely focuses on the crystal engineering of the high-quality thin MOF films and their application in gas separation. In particular, we focus on studies that highlight or

Received: October 19, 2018
Revised: November 30, 2018
Published: December 6, 2018

DOI: 10.1021/acssuschemeng.8b05409
ACS Sustainable Chem. Eng. 2019, 7, 49−69

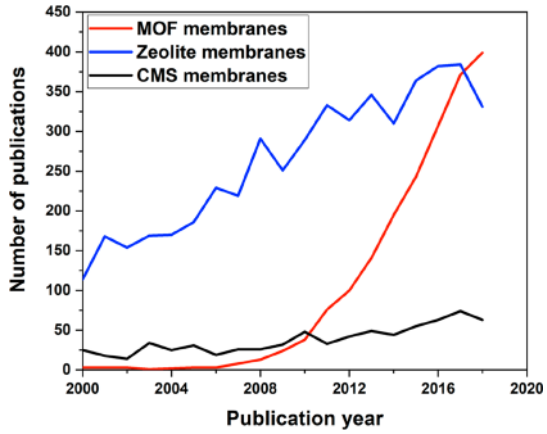

Figure 1. MOF membranes have quickly risen as the most promising nanoporous membranes. The plot compares yearly publications on MOF membranes with that on zeolite and carbon molecular sieves (CMS) based membranes. Data obtained from Web of Science until Oct 7, 2018.

exploit the role of nucleation, growth, and resulting grain properties. Although, there are several excellent reviews on the synthesis and application of MOFs,[7,19−24] especially for energy-efficient separations, this perspective is unique with its focus on morphology engineering for polycrystalline MOF films. First, we briefly discuss the MOF growth mechanism and how can one take insights from growth mechanism to develop high-quality films (nucleation and growth of MOFs section). Then, we dive into the key elements for the synthesis of MOF films with a discussion about crystal engineering, control over film morphology, role of lattice-flexibility, solvents and defects in MOF membranes, and postsynthetic modifications. Finally, we discuss the state-of-the-art for MOF based gas separation membranes and conclude by highlighting opportunities and challenges for the MOF membranes.

NUCLEATION AND GROWTH OF MOFS

The crystallization studies on polycrystalline MOF films have been heavily influenced by the crystal engineering knowledge generated on zeolites, mainly because (i) both zeolite and MOFs are microporous crystals with permanent porosity, and can be synthesized by almost similar solvothermal processes, and (ii) several successful zeolite growth and morphology engineering preceded MOF discovery. As a result, the early developments in the MOF films benefited from the expertise in the synthesis of zeolite films at comparatively harsher synthesis conditions. Despite this particular evolution, it is important to make key distinctions between MOFs and zeolites from the point of view of their structural chemistry and the synthesis mechanism. Unlike zeolites, which are covalently bonded, MOFs are composed of a weaker coordination bond between an organic linker and a metal node. This difference in chemical structure is also reflected in the growth mechanism and the related kinetics. While there has not been a universally agreed model for the zeolite growth, the most commonly attributed model for zeolite growth is a nonclassical growth mechanism where growth accompanies the formation of an amorphous gel where a combination of primary and secondary building units as well as precursor nanoparticles participate in the growth.[25−27] In contrast, the amorphous gel is usually not observed in the synthesis of MOF, although, in several cases, precursor nanoparticles mediated growth[28] as well as amorphous to crystalline transition[29] have been reported (e.g., ZIF-8, Figure 2).

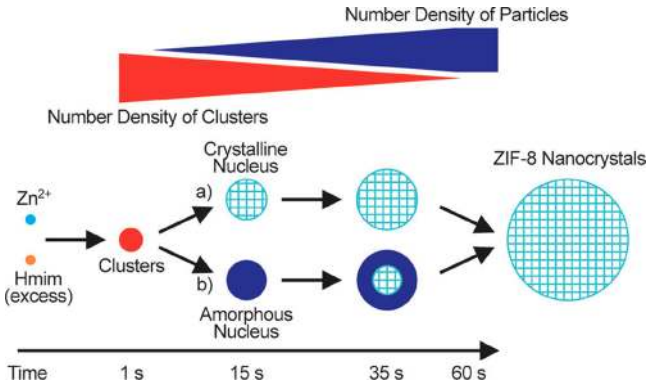

Figure 2. Schematic of the nucleation and growth pathway of ZIF-8 nanocrystals under conditions of high supersaturation. Reprinted with permission from reference 28. Copyright 2011 John Wiley & Sons, Inc.

Moreover, depending upon structure and the reaction parameters, both classical nucleation where small (relative to nuclei size) solvated complexes composed of ligand coordinated metal ions attach to the growing MOF as well as nonclassical growth involving aggregation, amorphous to crystalline transformations, dissolution-recrystallization and solid phase transformations have been observed for MOFs. A recent review by Schmidt and co-workers provides a comprehensive review on the experimental and computational studies on MOF nucleation and growth.[30]

Solvothermal reactions, in general, are governed by both chemical parameters (nature and composition of the reactants, pH, type of the solvents) and thermodynamic parameters like temperature and pressure.[31] Critical to the development of a high-performance membrane is the control over nucleation, growth and thickness. The nucleation and growth of MOFs have been predominantly modeled using the Avrami-Erofeev[32] (AE, eq 1) and the Gualtieri models[33,34] (eq 2).

$$\alpha = 1 - \exp(1 - (kt)^n) \tag{1}$$

$$\alpha = \frac{1 - \exp(1 - (k_G t)^{n_G})}{1 + \exp\left(-\frac{t - a_N}{b_N}\right)} \tag{2}$$

where α refers to the crystallization degree (0 being amorphous, and 1 being fully crystalline), k is the growth rate constant, t is growth time, and n is the Avrami exponent. In eq 2, k_G is the growth rate constant, n_G is the dimensionality of crystal growth, a_N is reciprocal of the nucleation rate constant, and b_N is the variance of the nucleation probability distribution. While the AE model, originally developed for solid-state phase transformation, does not distinguish between nucleation and growth events, the Gualtieri model was constructed to describe the solution-mediated crystallization. For instance, the relative magnitudes of $1/a_N$ and k_G can indicate whether the nucleation or the growth is the rate-determining process. Interestingly, the magnitude of b_N can indicate nature of nucleation with a crossover from the primarily homogeneous nucleation to the primarily heterogeneous nucleation.[33,34] Therefore, by systematically modeling the crystallization as a function of growth conditions, one can engineer the nucleation and growth stages

DOI: 10.1021/acssuschemeng.8b05409
ACS Sustainable Chem. Eng. 2019, 7, 49−69

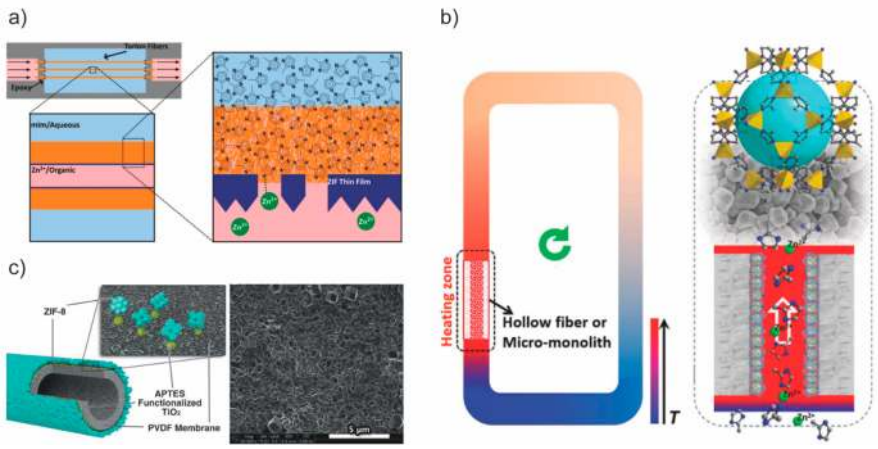

Figure 3. (a) Left: Schematic illustration of a microfluidic approach to grow ZIF-8 layers on hollow-fibers. Zn^{2+} ions are supplied in a 1-octanol solution (light red) flowing through the bore of the fiber and methylimidazole linkers are supplied on the outer (shell) side of the fiber in an aqueous solution (light blue). Right: Magnified view of the hollow-fiber's cross section during synthesis. Reprinted with permission from reference 44. Copyright 2014 American Association for the Advancement of Science. (b) Left: Illustration of the convective circulation synthesis loop to form a defect-free MOF layer on the inside of a hollow-fiber. Right: ZIF-8 membrane formation process in the fiber lumen. Reprinted with permission from reference 46. Copyright 2018 John Wiley & Sons, Inc. (c) Left: Schematic illustration of the ZIF-8 membrane formed on an APTES-TiO_2 modified PVDF support. Right: SEM image of the surface morphology of the intergrown ZIF-8 membrane. Reprinted with permission from reference 49. Copyright 2016 John Wiley & Sons, Inc.

of a MOF film. For example, one could conduct experiments to study induction time, nucleation density, and the dependence of α with respect to pH, temperature, linker and metal ion concentrations, promoter concentration, etc. The resulting data will help determine $1/a_N$ and k_G as a function of the growth conditions, and therefore one can choose a nucleation dominated regime or a growth dominated regime to engineer a high-quality film.

The nucleation event has been shown to be controlled by the ratio between the linker and the metal ions. Generally, the nucleation density tends to be higher when linker to metal-ion ratio in the growth sol is higher.[35−37] The evolution of ZIF-8 crystallization chemistry provides an interesting insight. The first report of ZIF-8 synthesis by Yaghi and co-workers used DMF as a solvent with a very low linker to metal ratio (<1).[38] Because the kinetic diameter of DMF (~5.5 Å) is larger than the pore window of ZIF-8, a successful membrane preparation required the substitution of DMF with smaller solvent molecules. Cravillon et al. found that by adding excess linker during the synthesis in methanol (linker to metal-ion ratio of 8), phase pure ZIF-8 nanocrystals could be obtained at room temperature.[35] Modifying this method with the addition of sodium formate during the solvothermal synthesis, Caro and co-workers synthesized the first polycrystalline ZIF-8 membrane in 2009.[39] Sodium formate promoted the heterogeneous nucleation and aided the crystal intergrowth,[40] which are crucial prerequisites in the synthesis of polycrystalline membranes. Later, by employing a very high ratio between linker and metal ions (70), Lai and co-workers developed an aqueous based synthesis method for ZIF-8 nanocrystals and membranes without using sodium formate.[41]

CRYSTAL ENGINEERING OF MOF FILMS

The synthesis routes for a high-quality polycrystalline film can be broadly classified into two categories; the *in situ* growth and the seeded secondary growth. While in the former method, the growth is one-step as the substrate is directly immersed in a growth precursor solution, the latter method by design is two-step, where the substrate is first coated with crystals to improve the control over film morphology (grain-boundaries, intercrystal voids, film-orientation, and thickness). In general, *in situ* growth is preferred over seeded secondary growth because the prior is less complex and reduces the number of steps to produce the final membrane. On the other hand, the latter provides a better control over the film morphology. In the following sections, key factors influencing these two routes, and the resulting structure−property relationship will be discussed.

***In Situ* Growth.** The main advantage of the *in situ* method is its high scale-up potential. The process is simple, however, obtaining a defect-free membrane by this route can be challenging, and often requires a rigorous optimization of the synthesis conditions. Here, it is important to guide the crystallization process to occur preferentially on the surface of the porous support and not in solution. Popular strategies to promote this are (i) functionalizing the support surface with an organic linker with an affinity for the metal ions, (ii) using an interfacial approach where the metal ions and linker molecules are dissolved in separate solutions and react at the interface, and (iii) coating the surface of the substrate with a metal oxide layer to increase the interaction with the ligands. This review will focus on a few recent examples that use variations of the *in situ* growth approach to achieve high performance MOF membranes. A detailed summary can be found in several excellent review papers.[20,42,43] In order to preserve the main advantage of using the *in situ* growth approach versus a seeding process, all the steps used to guide the MOF growth in the surface should be as simple and scalable as possible. In addition, they should be as broad as possible to be useful for different porous substrates and with different MOFs.

For the *in situ* crystallization of MOF film from a precursor solution, it is extremely important to promote the heterogeneous nucleation on the substrate. Typically, nucleation and growth are not decoupled, and the overall film growth involves simultaneous heterogeneous nucleation and growth. The

DOI: 10.1021/acssuschemeng.8b05409
ACS Sustainable Chem. Eng. 2019, 7, 49−69

density of heterogeneous nucleation determines the minimum possible thickness of a defect-free polycrystalline film. Nair and co-workers demonstrated a microfluidic approach capable of guiding the growth of the MOF layer in any desired location of a hollow-fiber (inner surface, outer surface, and even in the bulk of the fibers).[44] Their process consisted of flowing one of the MOF precursors (i.e., metal ions or organic linker) in the shell side and the other one in the core of the hollow-fiber. The reaction front pins at the interface where these two solutions meet (Figure 3a). By controlling the reactant flow profiles, concentrations, and temperature, they were able to guide the growth in different parts of the hollow-fiber, and achieved high-performance membranes with a C_3H_6/C_3H_8 separation factor of 90 at 9.5 bar.[45] Recently, Huang et al. also developed a method to synthesize a selective MOF film by flowing the reactants inside a hollow-fiber.[46] However, in their approach, both reactants were supplied together, and the growth of the MOF film was controlled via a convective circulation method (Figure 3b). These approaches are advantageous because the growth is done in one-step, and can be potentially carried out inside a hollow-fiber module, avoiding the risk of forming cracks during membrane handling.

To promote the heterogeneous nucleation, a popular route is substrate modification with chemical groups or metal oxide layers, increasing interactions with the metal ions and/or ligands. Coincidently, similar synthesis principle is also embodied by biomineralization, where a protein directs the crystallization of an inorganic film (e.g., seashell).[47] The essence of this concept is to enrich the precursor in the vicinity of the substrate, increasing the local concentration of the reactants, and thereby facilitating an efficient heterogeneous nucleation. Using this principle, Peinemann and co-workers synthesized a thin ZIF-8 film on a metal chelating polythiosemicarbazide (PTSC) support.[48] The chelating capability of the PTSC afforded a high density of zinc ions at the support surface, facilitating a uniform heterogeneous nucleation of ZIF-8 on the support. Chen and co-workers employed simultaneous modification of chemical structure and morphology of the substrate to promote ZIF-8 heterogeneous nucleation on polyvinylidene fluoride (PVDF) hollow fibers. The polymeric substrate was coated with (3-aminopropyl)-triethoxysilane (APTES) functionalized TiO_2 nanoparticles to improve heterogeneous nucleation (Figure 3c).[49] The amino groups complexed with the zinc ions in the growth solution, promoting the nucleation density. The high surface area TiO_2 coating seemingly improved the bonding between the substrate and the ZIF-8 film. A 400 nm-thick, pinhole-free ZIF-8 film was synthesized by immersing the modified support in the growth solution for several hours. Strategies that use metal oxide layers or metal-rich deposits to promote the heterogeneous nucleation can also minimize, or even eliminate, the use of solvents. Li et al. demonstrated that by doing a sol−gel coating of a Zn-based gel in the surface of a porous support and further exposing it to 2-methylimidazole vapor they could form continuous, defect-free ZIF-8 membranes that showed an outstanding performance.[50] This strategy produced the thinnest polycrystalline ZIF-8 membrane reported to date, and the authors demonstrated the fabrication of a module as a proof of principle for its scalability. In a recent report, Tsapatsis and co-workers completely eliminated the use of solvents and fabricated the first ZIF membrane using an all-vapor-phase processing method.[10] They use ALD to deposit ZnO in a α-alumina macroporous substrates coated with a ~5 μm γ-alumina mesoporous layer with pores in the 2 to 5 nm range followed by ligand-vapor treatment to partially convert the ZnO to ZIF. An all-vapor method is highly attractive and the performance of the reported membranes is one of the best reported so far for C_3H_6/C_3H_8.

Generally, most of the methods employ substrate modification to improve heterogeneous nucleation. Although this has proven extremely useful to synthesize high-quality MOF films, such approaches increase the complexity of the process as well as the cost of the resulting membranes. Keeping this in mind, recently our group reported a novel route termed as electrophoretic nuclei assembly for crystallization of highly intergrown thin-films (ENACT), capable of synthesizing high-quality thin MOF films on as-received, unmodified porous and nonporous substrates (Figure 4).[51,52]

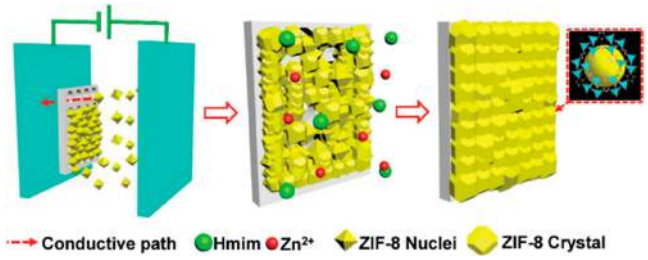

Figure 4. Illustration of the ENACT process that promotes the heterogeneous nucleation over a substrate by means of electrophoretic deposition directly from a growth precursor solution. Reprinted with permission from reference 51. Copyright 2018 John Wiley & Sons, Inc.

The ENACT route utilizes an external electric field to direct MOF nuclei onto a substrate that is attached to an electrode. The charged nuclei drift toward the electrode with a flux that is proportional to the strength of applied electric field (E), electrophoretic mobility of colloid (μ) and concentration of nuclei (C_n) as per Equations 3 and (4).

$$\text{Nuclei Flux} \propto E\mu C_n \tag{3}$$

$$\mu = \frac{v}{E} = \frac{\varepsilon_0 \varepsilon_r \zeta}{\eta} \tag{4}$$

where v is the drift velocity, ζ is the zeta potential of the colloid, ε_0 is permittivity of vacuum, ε_r is the dielectric constant and η is the viscosity of the dispersing medium. In the case of ZIF-8, a 100 nm-thick and compact film, consisting of 10−20 nm sized nuclei, could be obtained on a porous alumina substrate by applying a small electric field of 100 V/m for a few minutes. The nuclei film was intergrown into a pinhole-free polycrystalline ZIF-8 film by simply soaking in a precursor growth solution. In addition, well-intergrown membranes could be realized on various substrates (ceramic, metal, carbon, graphene), irrespective of their porosity (porous as well as nonporous), conductivity (conductive as well as nonconductive), and chemistry (ZIF-8 as well as ZIF-7).

Seeding for the Seeded Secondary Growth. An ideal crystallization chemistry for the synthesis of polycrystalline membranes should allow one to synthesize a defect-free membrane with an independent control over grain-size, membrane thickness and orientation while eliminating pin-

DOI: 10.1021/acssuschemeng.8b05409
ACS Sustainable Chem. Eng. 2019, 7, 49−69

holes. Seeding followed by secondary growth, a concept borrowed from zeolite membranes, is a common method for obtaining a well-intergrown, thin, defect-free MOF membrane. By decoupling the nucleation and the growth process, this method offers greater control over grain size, membrane thickness and orientation when compared to a direct growth process. Critical to the success of this route is the generation and attachment of a high density of small crystals (seeds) on a chosen substrate. Several techniques for seeding have been reported over the years ranging from manual rubbing of the seeds to chemical modifications of the surface. These techniques with their advantages and challenges are discussed briefly in this section.

Manual rubbing of the presynthesized seeds on to the substrate is one of the simplest and earliest seeding techniques used for the successful synthesis of MOF membranes.[53−55] Interestingly, the ZIF-8 membrane prepared by Venna et al.[55] had a very high CO_2 permeance of 2.4×10^{-5} mol m^{-2} s^{-1} Pa^{-1}. However, because of the poor adhesion between the substrate and the MOF layer, the membrane could withstand only a transmembrane pressure of ∼1.4 bar. To improve the adhesion between the MOF layer and the substrate as well as to promote heterogeneous nucleation, a commonly used strategy is the chemical modification of the substrate. Poly(ethylenimine) (PEI) enhances the adhesion of the seeds to the substrate surface by means of hydrogen bonding[56] as well as by the formation of Zn−N coordination bonds to zinc cations on the surface of the crystal.[57] PEI modification has been used for the synthesis of randomly oriented ZIF-7[56,58] membranes as well as oriented ZIF-8,[59] ZIF-7[60] and ZIF-L[57] membranes. Because of its ability to bind to all kinds of organic and inorganic surfaces through the formation of strong covalent and noncovalent bonds, polydopamine (PDA) is another compound widely used for surface modification of porous supports for membrane fabrication. Caro and co-workers reported the first use of PDA for membrane synthesis in 2013,[61] and since then the method has been extended to the synthesis of different MOF membranes on a wide variety of substrates.[62−64] A recent review has summarized the use of dopamine for membrane-based applications.[65] APTES modification of the support is another commonly employed route for obtaining a good seed layer. APTES act as a covalent linker between the MOF layer and the support. Huang et al. reported the successful synthesis of ZIF-8, ZIF-22 and ZIF-7 membranes using this approach.[66] The amine groups in APTES is assumed to coordinate to the free Zn^{2+} sites and bind the crystals on to the substrate.[49,67] In the case of ZIF-90, the APTES act as a covalent linker between the ZIF-90 layer and the alumina support via imine condensation.[67] In the thermal seeding technique, a chemical bond is directly established between the support and the MOF layer without the usage of any additional chemical compounds. In this method, the crystal seed solution (or the linker solution) is deposited at high temperature on to a hot porous substrate. This technique has been demonstrated for the synthesis of HKUST-1,[68] ZIF-7[69] and ZIF-8[69] membranes.

Microwave assisted techniques have been used both as a seeding method as well as for the *in situ* growth.[39,70−72] The highly localized yet rapid and intense heating by microwave method promotes heterogeneous nucleation over the undesirable homogeneous nucleation in solution. Kwon et al. reported the synthesis of a dense seed layer of ZIF-8, ZIF-7 and SIM-1 with good adhesion to the substrate by microwave assisted seeding.[70] In their method, the porous support was first saturated with a metal precursor solution that was later transferred to a ligand precursor solution. Because of the high concentration of metals and ligands in the vicinity of the support, rapid crystal formation occurs under microwave irradiation. The presence of the metal precursor solution in the pores of the support aids in the rapid rise of temperature of the support surface as well. This leads to the formation of crystals in the pores of the substrate, which significantly enhances the adhesion of the MOF layer. Though microwave assisted techniques can significantly cut down the synthesis time, the requirement for an enclosure as well as microwave-compatible substrate, limits its applicability.

Engineering Growth Kinetics. The growth kinetics of polycrystalline film is mainly governed by the concentration of precursors (metal and ligand), temperature, solvent and additives. When tuning these parameters to improve the growth kinetics, one principal design concept that should be kept in mind is that the growth kinetics on substrate surface should be promoted while the concurrent homogeneous nucleation in the solution should be impeded. Moreover, a too fast growth kinetics is likely to generate crystal defects, while a slow growth is time-consuming and undesirable.

The precursor concentration (metal or ligand) in the solution is usually maintained at a low value to impede the homogeneous nucleation. If the concentrations of the metal ions and the ligand are high, a large number of nuclei would be formed in the solution, which can rapidly consume the precursor and hinder the film growth before a highly intergrown film is achieved. In this respect, Lai and co-workers reported one of the most popular recipe for ZIF-8 film growth.[73] The concentration of zinc nitrate was kept extremely low (9.2 mmol/L) while the ratio of 2-methylimidazole to zinc nitrate was kept at 70. The low concentration conditions effectively hindered the homogeneous nucleation while promoting the seeded secondary growth, leading to the formation of a defect-free, ZIF-8 film. By this method, they synthesized a 2.2 μm-thick ZIF-8 membrane in 6 h on a preseeded alumina support, which at that point of time, was almost 10 times thinner than other reported ZIF-8 membranes.[39]

A continuous supply of linker and metal ions during the secondary growth could become a promising strategy for decreasing both the membrane thickness as well as synthesis time. Instead of the classical secondary growth process in which the membrane is immersed in a precursor solution for an extended period of time, in a continuous process, the metal and the linker solutions are mixed just before introducing it on to the membrane surface in a continuous manner. Recently Wang et al. reported a synthesis method for obtaining monodispersed, size specific MOF crystals using controlled-nucleation-growth strategy (Figure 5a,b).[74] By separately delivering the metal and the ligand solutions to the reaction system in a controlled manner, the supersaturation degree could be controlled, which, in turn, delineates the nucleation and the growth phase. Because supersaturation degree for crystal growth is found to be lower than that for nucleation, fresh nucleation could be suppressed while promoting the crystal growth. The continuous supply of reactants ensures a balance between the supply and the consumption of the monomers. The authors reported the successful synthesis of different types of MOFs including ZIF-8, ZIF-67, MIL-100(Fe), MIL-101(Fe), MOF-801 and UiO-66. This

DOI: 10.1021/acssuschemeng.8b05409
ACS Sustainable Chem. Eng. 2019, 7, 49−69

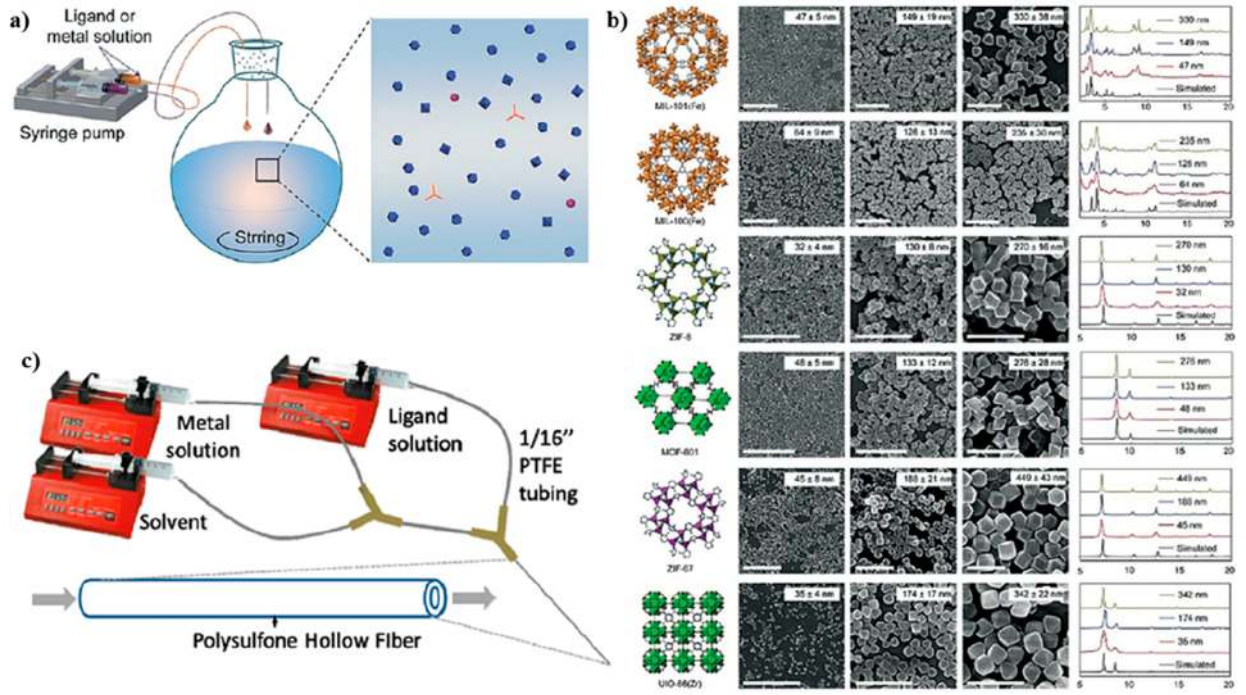

Figure 5. (a) Schematic of the reactor setup used for obtaining a precise size controlled monodispered MOF crystals. (b) SEM images of different MOF crystals prepared by this approach. Reprinted with permission from reference 74. Copyright 2018 John Wiley & Sons, Inc. (c) Schematic of a microfluidic setup used for preparing ZIF-8 and ZIF-7 membranes inside a polysulfone hollow fiber. Reprinted with permission from reference 75. Copyright 2015 Elsevier.

technique could be extended to the synthesis of polycrystalline membrane where in the homogeneous nucleation in the solution could be suppressed while promoting the growth of the seed crystals on the support. The closest analogy to this method reported for membrane growth is the microfluidic approach of Coronas and co-workers.[75] As shown in Figure 5c, they used three syringe pumps to deliver the metal, ligand and solvent solution to the interior of a polysulfone hollow-fiber and reported the successful synthesis of ZIF-8 (3.6 μm) and ZIF-7 (2.4 μm) membrane. Both the ZIF-8 and ZIF-7 membranes exhibited above Knudsen separation except for H_2/CO_2. However, the H_2 permeance was very low for both ZIF-8 (4.7×10^{-9} mol m^{-2} s^{-1} Pa^{-1} and ZIF-7 (2.15×10^{-9} mol m^{-2} s^{-1} Pa^{-1}) partly due to the very low permeance of the hollow fiber support itself (8.2×10^{-8} mol m^{-2} s^{-1} Pa^{-1} for H_2). In light of the recent report by Wang et al.,[74] we speculate that there is scope for significant improvement of membrane performance by this route, which not only saves reagent and time but may also pave the way for a continuous production of MOF powders and membranes.

CONTROL OVER FILM MORPHOLOGY (THICKNESS, CRYSTAL ORIENTATION AND GRAIN-BOUNDARIES)

One of the key design parameters of polycrystalline membrane is its thickness because it is expected to follow an inverse relationship with the molecular permeance and therefore can reduce the required membrane area and the capital cost. As a result, this has been the objective of the majority of the studies on MOF membranes. Naturally, a high control over the crystallization process is of paramount importance to achieve a thin, pinhole-free MOF film. Before venturing in this subject any further, it is important to note that the thickness–permeance relationship is not completely straightforward when dealing with polycrystalline MOF membranes. A performance comparison of the reported ZIF-8 membranes suggests that thickness is just one of the many factors determining whether a polycrystalline MOF membrane will achieve a high permeance. Figure 6 shows the relation between the H_2 permeance and selective layer thickness for several ZIF-8 membranes that have shown a clear molecular

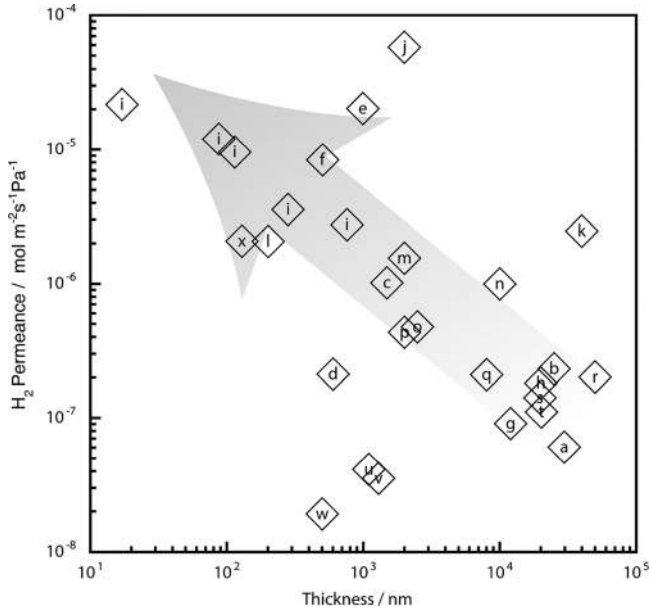

Figure 6. Observed thickness-permeance relationship in the reported ZIF-8 membranes. The letters a to x in the figure correspond to the references 39, 40, 46, 48, 49, 51, 59, 61, 50, 76–90, respectively.

DOI: 10.1021/acssuschemeng.8b05409
ACS Sustainable Chem. Eng. 2019, 7, 49–69

sieving capability (i.e., ideal H_2/CH_4 or H_2/N_2 selectivity of more than double of the corresponding Knudsen selectivity). Interestingly, the trend is not as clear as one expects. Membranes with a similar thickness yielded H_2 permeances that vary by more than 2 orders of magnitude, and vice versa, membranes with 2 orders of magnitude difference in thickness presented similar permeances. However, the best membranes reported so far are also some of the thinnest ones, especially those with a thickness below 500 nm. In fact, the trend is more clear when the thickness is lower than 500 nm. To the best of our knowledge, the thinnest ZIF-8 membrane ever made had a thickness of ca. 17 nm.[50] This particular membrane showed an outstanding performance at least in the terms of permeance: H_2 permeance of 215.4×10^{-7} mol m^{-2} s^{-1} Pa^{-1} with an ideal H_2/CH_4 selectivity of 18, and C_3H_6 permeance of 8.4×10^{-7} mol m^{-2} s^{-1} Pa^{-1} with a C_3H_6/C_3H_8 ideal selectivity of 44.

This variation in membrane permeance for a given thickness can be partly explained by the support resistance, and whether or not the MOF film crystallized inside the support. The transport across the support adds resistance to the overall transport, and in certain cases, support transport can limit the overall permeation. Therefore, great care must be taken when choosing the support, especially when the target is to synthesize sub-500 nm thick membranes. On the other hand, MOF can grow inside the support pores, increasing the effective thickness of the MOF film. Therefore, an accurate estimate of membrane thickness should account for the growth of MOF inside the support, especially when the support pores are smaller than 100 nm, where the probability of pore-plugging by the growing MOF crystal is high. Interestingly, plugging the support pores with MOF crystals can result in the formation of high-performance membranes. Recently, Tsapatsis and co-workers demonstrated a vapor-phase synthesis leading to extremely thin membranes where part of the ZIF-8 film was confined within the small 2- to 5 nm pores of a γ-alumina support.[10] Surprisingly, the not well-crystallized ZIF deposit confined inside the pores and surrounded by unreacted ZnO grains, generated one of the most promising membranes for the debottlenecking of propylene-propane distillation columns. Such synergistic arrangement of the γ-alumina support with small pores, the ZnO particles and ZIF crystals along with the complex grain-boundaries involved in such system were crucial for achieving a high C_3H_6 permeance and maintaining a good C_3H_6/C_3H_8 mixture selectivity even at pressures of 7 atm.

The presence of grain-boundary defects in a polycrystalline film is expected to affect the performance of the film. Understanding the role of grain-boundaries in MOF membranes and controlling them is still in its infancy. Recently, by employing an ultralow dose of electrons and an electron-counting camera in an aberration-corrected transmission electron microscope (ac-TEM), Han and co-workers, for the first time, reported atomically resolved images of ZIF-8, including the interface between two intergrown ZIF-8 crystals.[91] Their observations suggest that the individual grains are terminated with the ligand and that at the interface, two ligand molecules adhere without any chemical bonds (more details in section: Role of Lattice Defects). Further experiments corroborated with molecular dynamics (MD) simulations concluded that there is a defect-driven structure–property relationship between interfaces and mass transport, and that in the particular case of ZIF-8, it has a greater effect when dealing with a large guest molecule. In order to realize the importance of the grain-boundaries in polycrystalline membranes, it is useful to revisit the research done in zeolite membranes; Newsome and Sholl comprehensively described the effect of the grain-boundary structure on the mass transfer in zeolite membranes,[92] and later Tsapatsis and co-workers demonstrated a very effective strategy to control grain-boundary defects.[93]

Because the MOF structure consists of a porous-network, the orientation of pores with respect to the substrate is expected to affect the separation performance. Caro and co-workers synthesized a ZIF-8 film with (100) orientation and observed a small increase in the H_2/CH_4 separation factor when compared with its nonoriented counterpart.[59] However, they discarded the preferential orientation as a possible explanation for this and concluded that it was due to an improved microstructure quality (i.e., a better intergrowth of the grains). Recently, Eddaoudi and co-workers used a liquid-phase epitaxy (LPE) approach to synthesize ZIF-8 membranes with a preferential orientation along the (100) direction perpendicular to the support.[89] Even though the membranes were thin (500–1000 nm), the permeance achieved was one of the lowest reported in the literature. Interestingly, a preferred orientation is not required for membranes based on ZIF-8, and the best performing ZIF-8 membranes are randomly oriented. However, the orientation control is expected to be important for other MOF structures; particularly for MOFs with an anisotropic pore-channel system. Moreover, the arrangement of oriented MOF crystals is expected to reduce grain-boundaries misalignments, and therefore, the grain-boundary defects. A recent review by Wöll and co-workers summarizes the available strategies to control the orientation of MOF films.[94] Out of these strategies, very few have been successfully applied to the synthesis of defect-free MOF membranes. Liu et al. has highlighted the most recent advancements for controlling the orientation in MOF membranes.[95] An example of a MOF structure where an oriented film is required to achieve a good performance is the $M_3(HCOO)_6$ family. This family of MOFs possesses a set of one-dimensional zigzag channels running along the crystallographic *b*-axis making it important to orient the channels perpendicular to the support surface to obtain a high permeance. Li and co-workers reported that the use of a Ni foam with Cu-rich oriented nano–microstructure arrays as a support for $Co_3(HCOO)_6$ membranes can guide the growth of the MOF crystals along the (101) direction.[96] They reported an ideal H_2/CO_2 separation factor of 11.6 with a H_2 permeance of 9.1×10^{-7} mol m^{-2} s^{-1} Pa^{-1} for their optimized oriented $Co_3(HCOO)_6$ membrane. Another MOF where orientation is important is NH_2-MIL-125, which has straight nanochannels along the *c*-axis. An oriented membrane of such material is expected to offer a reduced diffusion barrier compared to its nonoriented counterpart. Recently, Sun et al. achieved the fabrication of *c*-oriented NH_2-MIL-125 membranes by using a combination of oriented seeding and microwave assisted in-plane epitaxial growth (Figure 7).[97] They used a layered TiS_2 as the metal source for synthesizing the oriented seeds and found that in order to intergrow the seeds into an oriented film it was indispensable to control the microwave field uniformity and intensity during epitaxial growth. The use of single-mode microwave irradiation yielded the required uniformity and intensity to promote the desired in-plane growth and suppress the undesired twin growth.

DOI: 10.1021/acssuschemeng.8b05409
ACS Sustainable Chem. Eng. 2019, 7, 49–69

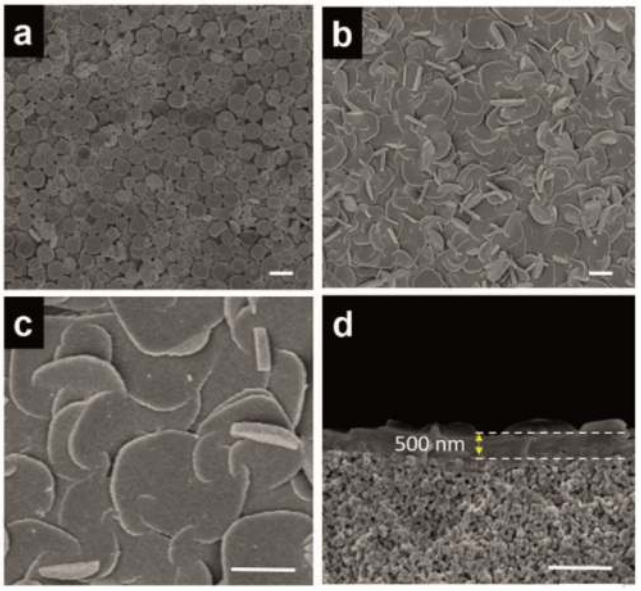

Figure 7. SEM images of the oriented NH_2-MIL-125(Ti) membrane. (a) NH_2-MIL-125(Ti) seed layer before the secondary growth; (b c) top-views, and (d) cross-sectional view of NH_2-MIL-125(Ti) membrane after secondary growth on the α-Al_2O_3 substrate. Scale bars: 1 μm. Reprinted with permission from reference 97. Copyright 2018 John Wiley & Sons, Inc.

Moreover, by comparing the gas permeation results of the *c*-oriented NH_2-MIL-125 membranes with the ones from their nonoriented counterpart,[98] it is clear that the oriented growth strategy is more effective in minimizing the grain-boundary defects. The *c*-oriented NH_2-MIL-125 membrane showed an ideal H_2/CO_2 selectivity of 25, while their randomly oriented counterparts showed a selectivity of only 4 with a H_2 permeability more than 1 order of magnitude higher at similar testing conditions.

ROLE OF LATTICE-FLEXIBILITY, SOLVENTS AND DEFECTS IN MOF MEMBRANES

Apart from the nucleation and growth kinetics, the key factors that affect the property of MOF membranes uniquely are the lattice flexibility, the solvents employed for the synthesis, and the lattice-defects. Below, we provide a short overview of these aspects.

Role of Lattice Flexibility. Unlike zeolites, MOFs may not exhibit a sharp cut off for the molecular sieving. Several MOFs seem to host molecules larger than the crystallographically determined pore aperture. This has been attributed to the lattice flexibility in these MOFs. The lattice flexibility has been observed for different MOF structures including but is not limited to ZIF-7,[99,100] ZIF-8,[101] ZIF-90[102] and MIL-53.[103] For bidentate linker based MOFs, this flexibility arises from the thermally activated flip/flop motion of the linker. Tridentate linker based MOFs, such as HKUST-1, are rigid. The curious phenomenon of lattice flexibility was intensively investigated by many research groups using different characterization approaches and came to the same conclusion. Of particular interest to gas separation applications is the case of ZIF-8. Using *in situ* high pressure single crystal XRD measurements, Cheetham and co-workers were one of the first to report the reorientation of the linker molecules of ZIF-8 leading to a more open structure at a very high pressure of 1.47 GPa.[104] A few years later, N_2 adsorption isotherm measurements at 77 K on ZIF-8 powders revealed two steps occurring at very low pressures of 0.002 and 0.02 bar that could be not be explained using a rigid model but fit perfectly by assuming a flexible structure.[105] Koros and co-workers investigated the molecular sieving properties of ZIF-8 using probes molecules of various sizes ranging from He (2.6 Å) to iso-C_4H_{10} (5.0 Å).[101] They observed a 10 orders of magnitude difference in diffusivity between C_3H_6 (4.0 Å) and iso-C_4H_{10}, and defined an effective-aperture-size in the range 4.0−4.2 Å (Figure 8a). Incidentally, the determined effective aperture size of ZIF-8 lies in a sweet spot for the separation of one of the most difficult and energy intensive separations in the chemical industry, the propane/propylene separation, thereby breathing a new life into MOF based gas separation studies. More intricate details of ZIF-8 framework flexibility were revealed in ^{2}H NMR spectroscopy and *in situ* inelastic neutron scattering studies (INS). ^{2}H NMR studies showed that the linkers of ZIF-8 are very mobile and exhibit 2-site flips (2θ = 34°) at a rate of ~10^{12} s^{-1} with a very low activation barrier of 1.5 kJ mol^{-1}.[106] Additionally, it was also found that the average position of the 2-methylimidazole linker does not lie in the plane of the ZIF-8 cavity window but occupies a tilted position of ±17° with respect to the window plane. The alternating linker positions (shown in Figure 8b) corresponds to an increase in the aperture size from 3.4 Å to ~4.0 Å, and is

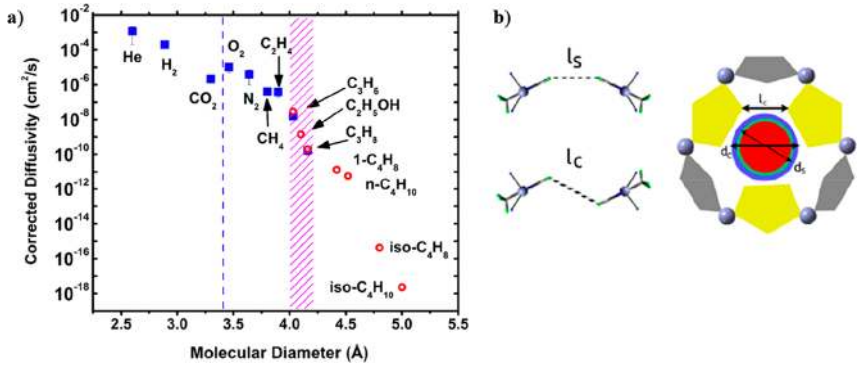

Figure 8. (a) Corrected diffusivity plot versus molecular diameter of various probe molecules depicting the effective aperture size of ZIF-8 to be about 4.0−4.2 Å. Reprinted with permission from reference 101. Copyright 2012 American Chemical Society. (b) Results from ^{2}H NMR studies on ZIF-8 indicating two possible orientations of the linker with respect to the window plane. The linkers occupying counter positions corresponds to a pore aperture size of 4.0 Å. Reprinted with permission from reference 106. Copyright 2015 American Chemical Society.

DOI: 10.1021/acssuschemeng.8b05409
ACS Sustainable Chem. Eng. 2019, 7, 49−69

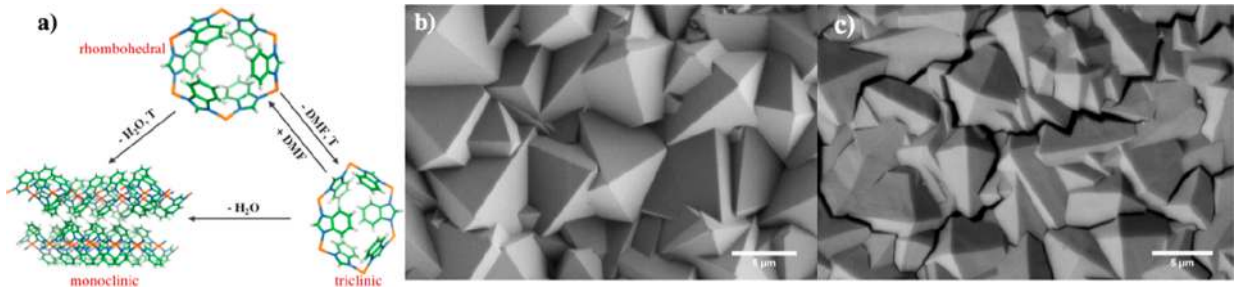

Figure 9. (a) Phase transitions observed in ZIF-7 (adapted with permission from reference 116). SEM image of ZIF-7 membrane (b) before activation and (c) after activation. Intercrystalline as well as intracrystalline cracks can be seen after the activation of the membrane.

in perfect accordance with the diffusivity studies of Koros and co-workers.[101] The swinging of the imidazolate rings upon N_2 adsorption was also confirmed with INS, which is sensitive to the dynamics of hydrogen and hydrogen bearing groups due to the relatively large incoherent neutron cross section of hydrogen.[107] The increased steric hindrance for methyl rotation caused by the swinging of the imidazolate rings resulted in a blue shift of the rotational transition peak in the INS spectrum by as much as 13.3 meV. By combining adsorption measurements with INS, it was also observed that molecules with strong quadrupole moment like CO and N_2 induce rotation of the linkers while adsorption of other molecules like Ar or O_2 did not lead to a rotation of the linkers but only produced a framework expansion at high relative pressures.[108]

To obtain a higher molecular selectivity, several approaches have been pursued by various research groups to restrict the framework flexibility in MOFs. The covalent functionalization of the linkers with a bulky functional group can restrict the flip−flop motion of the linkers. Huang et al. achieved a very high H_2/CH_4 selectivity of 71 by postsynthetic covalent functionalization of ZIF-90 with the bulky APTES.[109] The amine group of APTES reacts with the aldehyde group in the ZIF-90 framework and results in a restricted linker motion leading to the observed higher H_2/CH_4 selectivity. Nair and co-workers have shown that by the substitution of the 2-methylimidazolate linker of ZIF-8 with the bulky benzimidazolate linker of ZIF-7, the lattice flexibility could be suppressed in the resulting ZIF-7−8 hybrid material.[110] The substitution of the metal nodes has also been shown to improve the separation performance due to a stiffening of the lattice. By preparing a sandwich structure of ZIF-8 and ZIF-67, Kwon et al. observed an increase in the propane/propylene separation factor, and attributed it to a stiffer Co−N bond (ZIF-67) compared to Zn−N bond in ZIF-8.[111] Recently, Caro and co-workers have shown that a high electric field (500 V/mm) can transform ZIF-8 framework into polymorphs with rigid structure resulting in an increase in the separation factor.[112] In a subsequent work, they were able to directly synthesize the distorted ZIF-8 phase (C_m) by a fast current-driven synthesis method. The distorted C_m phase accounted for 60−70% of the membrane composition resulting in the highest reported propylene/propane separation factor of 305, and with a corresponding C_3H_6 permeance of 5 GPU.[113]

The chemical composition and the morphology of the porous support is also found to influence the lattice flexibility. To the best of our knowledge, there is no systematic study on substrate effect on lattice flexibility; however, it is likely that confinement of MOF grains within the substrate or over the substrate restricts the lattice flexibility. For example, Huang et al. reported a bicontinuous ZIF-8-graphene-oxide (ZIF-8-GO) layer prepared by the layer-by-layer deposition of GO on a discontinuous ZIF-8 layer.[114] The gaps between the discontinuous ZIF-8 layer were filled by the deposited GO and resulted in very high ideal selectivities of 22 (H_2/CO_2), 104 (H_2/N_2) and 198 (H_2/CH_4). The lateral constriction of the ZIF-8 lattice by the rigid GO layer was pointed out as the reason for the observed high selectivities. Shamsaei et al. prepared a 200 nm-thick ZIF-8 membrane on a polydopamine coated carbon nanotube (CNT) modified porous support.[62] Ideal gas selectivities higher than typically reported for ZIF-8 were observed: 14 (H_2/CO_2), 18 (H_2/N_2) and 35 (H_2/CH_4). Zhang et al. prepared a freestanding ZIF-8 membrane (~550 nm) on a polydopamine modified single walled CNT film.[64] ZIF-8 layers were formed on both sides of the CNT interlayer and exhibited a high H_2/CO_2 ideal selectivity of 43. Curiously, the H_2/N_2 (20) and H_2/CH_4 (38) selectivities were found to be lower than the H_2/CO_2 selectivity. Because the kinetic diameter of CO_2 is smaller than those of N_2 and CH_4, the higher H_2/CO_2 selectivity could be because of a strong adsorption of CO_2, constricting the transport pathway.

Role of Solvent. For any solution-based crystallization approaches, the choice of solvent is of paramount importance. Li and Du have reviewed the role of solvents in the synthesis of coordination compounds.[115] In the synthesis of polycrystalline films, in addition to the solubility, reaction kinetics and thermodynamic considerations, the size of the solvent molecule has also to be taken into account. Large molecules like DMF are difficult to remove from MOFs with aperture size smaller than the kinetic diameter of the solvent molecule. This typically leads to the formation of cracks upon solvent removal on otherwise well-intergrown defect-free films. The role of solvents in the synthesis of a polycrystalline membrane for gas separation is very interesting in the case of ZIF-7. DMF is the solvent that is typically used for the synthesis of ZIF-7 resulting in a rhombohedral phase.[38,56] Zhao et al. have shown that a complete removal of DMF from ZIF-7 induces a phase transition to a triclinic structure, which is found to revert to the rhombohedral structure upon reimmersion in DMF (Figure 9a).[116] When the DMF is exchanged with water and heated to above 400 K, a nonporous monoclinic structure is obtained. The triclinic phase also transforms irreversibly to the monoclinic phase upon immersing in water for several days. In our experiments, we have invariably observed the cracking of the membrane structure and associated phase change upon activation (Figure 9b,c). Thus, at least in the case of ZIF-7, the solvent plays a similar role as structure

DOI: 10.1021/acssuschemeng.8b05409
ACS Sustainable Chem. Eng. 2019, 7, 49−69

directing agents (SDA) for zeolites. The different phases of ZIF-7 have distinct pore apertures ranging from 2.1 Å for the monoclinic phase to 3.0 Å for the rhombohedral phase. In gas separation by molecular sieving, where a sub 0.2 Å changes in pore apertures can lead to significant changes in diffusivity, ZIF-7 represents the extreme case. A nonsolvent induced transformation leading to similar changes of pore aperture (e.g., by external stimuli) have promising potential for a tunable gas separation molecular sieve membrane.

Role of Lattice Defects. Defects in MOFs have garnered increasing attention in recent years and have been the subject for a number of recent reviews. Sholl and Lively gave an excellent perspective summarizing the developments in the understanding of the defects in MOFs.[117] Fischer and co-workers discussed the different characterization techniques used for identifying defects in various MOFs,[118] and Coudert and co-workers laid out an interesting picture of how defects, disorder, and flexibility are inescapably intertwined.[119] Recently, Dissegna et al. summarized the recent progress in the understanding and application of defective MOFs.[120] However, in the field of MOF-membrane-based separation processes, the role of defects is often overlooked and confused with the flexibility of the framework. Defects in MOFs, like in any crystalline material, can be in the form of point defects (linker/metal vacancies), line defects (dislocations), planar defects (grain-boundaries/stacking faults) and volume defects (pinhole/cracks). Compared to linker vacancies, instances of metal vacancies are rather rare in MOFs. Linker vacancies occur naturally during the crystal formation phase or can be intentionally created. Rapid crystallization during the synthesis is one of the reasons for the formation of linker vacancies.[121−123] Ravon et al. studied defects in MOF-5 synthesized by a fast precipitation process, by Fourier transformed infrared spectroscopy (FTIR), where they observed the formation of the Zn−OH species.[123] The presence of these defect sites is known to improve the catalytic activity of MOF. However, for the separation processes, the presence of such defective sites deteriorates the membrane performance. Lee et al. investigated the stability of ZIF-8 membranes synthesized by the counter-diffusion and the microwave/solvothermal methods.[122] Because of the shorter synthesis time for the counter-diffusion process, the membrane obtained was found to be more defective than the one prepared by the microwave/solvothermal method. Long-term stability measurements carried out over a period of 60 days revealed that the permeance of the more defective membrane decreased by as much as 75% of its initial value while for the less defective one, the decrease was only 25%. A subsequent treatment of the defective membrane in a ligand solution was found to improve the long-term stability. Postsynthetic exposure of MOFs to corrosive gases can also lead to the formation of defects in the crystal. Bhattacharyya et al. have shown that even ppm concentration of humid SO_2 can cause significant damage to the ZIF-8 framework over time, due to the cleavage of Zn-imidazole bond.[124] In a subsequent study, they reported a method to recover degraded ZIF-8 crystals by exposing them to a linker solution under the solvothermal conditions.[125] Using deuterated linkers they found that the recovery of the material is not a simple acid−base exchange process but actually occurs through a complete replacement of the old linker-acid defect complex with a brand-new linker.

Grain-boundary defects contribute significantly to the overall mass transport, especially when the grain size decreases to less than a micron, increasing the overall concentration of the grain-boundary defects. However, the understanding of grain-boundary defects in MOF is still in the nascent stage, mainly because observing their structure by electron microscopy is impeded by the inherent vulnerability of MOFs to the electron beam. It should be noted that the grain-boundary defects are extremely difficult to analyze by spectroscopic techniques because of the limited spatial resolution and sensitivity of the available techniques. Recently, Han and co-workers reported a pioneering development where lattice-resolved images of ZIF-8 were obtained using a low beam-dosage condition and an electron-counting camera.[91] They observed the interface of intergrown ZIF-8 crystals and reported a coherent orientation with a perfect alignment of the two grains attributing to the directional H-bonding between the terminal ligands. In addition, the separation of the two crystals was determined to be ∼0.4−0.6 nm, corresponding to an additional layer of ligands at the interface with respect to the perfect crystal structure as shown in Figure 10. We think that the presence of this terminal linker only channel can, in principle, offer a space for individual crystals to expand upon heating or guest loading, leading to an additional source of flexibility. It should be noted that the above description of grain-boundary is only valid for two coherent crystals oriented along the (110) surface. In polycrystalline membranes, the crystals are often randomly oriented and the intergrowth of the two randomly oriented crystals could paint a different picture. Nevertheless, this picture presents opportunities to engineer grain-boundary defects by either substituting the linker at the grain-boundary or by utilizing the under-coordinated site on the linker in the grain-boundary.

POSTSYNTHETIC MODIFICATIONS

Healing Lattice Defects. One of the most straightforward methods for reducing or eliminating the defects in the polycrystalline membrane is by carrying out a regrowth (multiple secondary growth). From our experiments, we have observed that reimmersion in the growth solution significantly reduces the defects in the MOF film while improving the reproducibility. However, the regrowth invariably results in an increase in the thickness of the MOF film accompanied by a decrease in the permeance. Another method for reducing the nonselective pathway in a MOF membrane is to apply a polymer to seal the defects. However, such surface modification could lead to pore blockage and hinder molecular transport resulting in a decreased overall permeance. Kwon et al. reported a defect induced ripening of ZIF-8 framework where a defective ZIF-8 membrane when exposed to ligand vapor, undergoes an Ostwald ripening process and the subsequent growth seals the defects in the membrane.[126] The ripening process was found to occur more readily on the rapidly synthesized membrane (more defective films) while the less defective membranes were found to be not as responsive to the ripening process. In addition, the presence of water was found to expedite the process indicating a synergistic effect of water vapor. The morphology change of the ZIF crystals exposed to ligand vapor was evident in the SEM images as the crystals grew in size and neck formation between crystals was also observed after the ripening. However, only one out of the three membranes showed an

DOI: 10.1021/acssuschemeng.8b05409
ACS Sustainable Chem. Eng. 2019, 7, 49−69

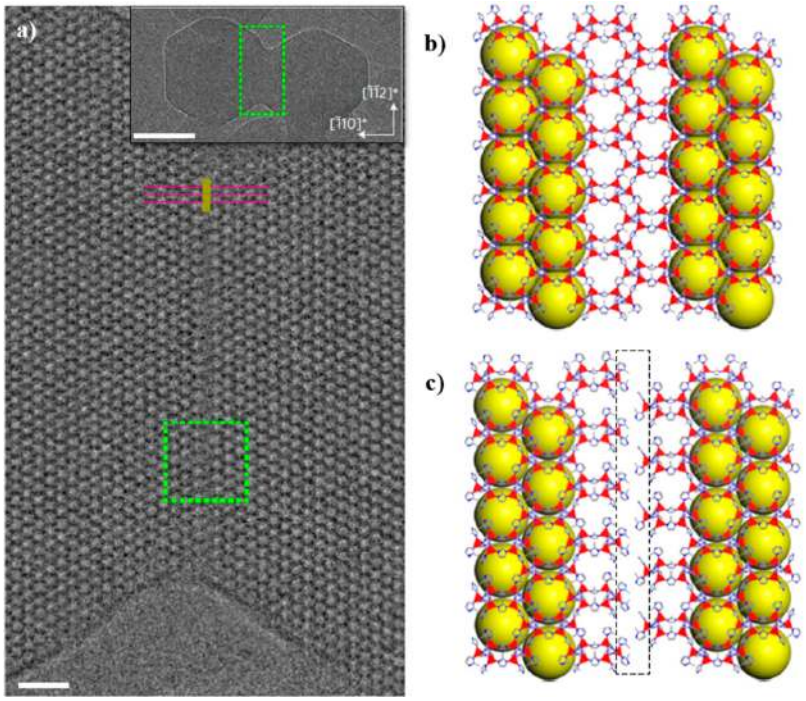

Figure 10. (a) Ac-TEM image of the coherent interface formed between two assembled ZIF-8 crystals (scale bar, 5 nm). Inset shows the low magnification image of the two oriented, intergrown ZIF-8 crystals (scale bar, 50 nm). Schematic of the (b) bulk and (c) interfacial structures of ZIF-8 lattice projected along the [111] direction showing the identical arrangement of lattice except for the existence of an additional layer of ligands in the interface denoted by the black rectangle. Reprinted with permission from reference 91. Copyright 2017 Macmillan Publishers Limited, part of Springer Nature.

enhancement in the propylene/propane separation factor. In a later work by the same group, a postsynthesis treatment of the membrane in an aqueous ligand solution was shown to reduce the defects and improve the stability of the ZIF-8 membrane.[122]

Linker-Exchanged MOF Films. One of the important characteristics of MOFs that distinguishes it from zeolites is its structural- or functional-tunability. The organic nature of the linkers in the MOFs and the underlying coordination chemistry paves a relatively easy way for linker functionalization and substitution. In general, there exist two different strategies for obtaining mixed linker MOFs-de Novo synthesis and postsynthetic linker exchange. In de Novo synthesis, the different linkers are mixed in the synthesis stage itself. Nair and co-workers did some pioneering works in de Novo synthesis of hybrid MOFs focusing their attention on ZIF-7, ZIF-8 and ZIF-90.[110,127,128] Both ZIF-8 and ZIF-90 have a cubic structure and a continuous composition distribution could be obtained by a de Novo synthesis strategy,[127] while for ZIF-7 incorporation in ZIF-90, a single solvent system was not capable of yielding a continuous composition variation.[128] It was also observed that the incorporation of the ZIF-7 linker (benzimidazole) can eliminate the framework flexibility. Solvent-assisted linker exchange (SALE) is the most common method for postsynthetic linker modification and has been demonstrated for various MOFs. An excellent review by Hupp and co-workers provides more details.[129] Using the SALE approach, even comparatively robust ZIF-8 was found to be susceptible to extensive linker exchange.[130] The 2-methylimidazole linker in ZIF-8 was substituted with imidazole linkers achieving almost 85% substitution in butanol. The absence of the methyl group in imidazole linker enlarges the aperture of the modified ZIF-8 (SALEM-2) leading to the uptake of larger molecules like toluene and cyclohexane. Recently, Jayachandrababu et al. used confocal fluorescence microscopy in combination with ^{1}H NMR, multiple pulse spectroscopy, and isotherm measurements to reveal the differences in the linker distribution between de Novo and SALE synthesized ZIF-8−90 framework.[131] The native fluorescence of the imidazolate linker was used to investigate the spatial distribution of the linkers in the resultant framework. When excited by a 405 nm laser, ZIF-8 emits blue light (460 nm) while ZIF-90 crystals emit green light (505 nm). While the de Novo synthesized crystals were found to be mixed at a unit-cell level, the SALE process leads to a core−shell morphology as shown in Figure 11a,b.

The linker exchange studies on polycrystalline films are scarce compared to powder-based studies, presumably due to the relative difficulty in obtaining a defect-free film. Recently Hillman et al. reported a de Novo synthesis route for obtaining a ZIF-7−8 hybrid structure.[71] The porous substrate was first immersed in a metal precursor solution for 1 h, which was later transferred to a mixed linker (methylimidazole and benzimidazole) solution followed by microwave irradiation for 90 s. The resulting membrane exhibited a H_2 permeance of 3 × 10^{-7} mol m^{-2} s^{-1} Pa^{-1} with a H_2/CH_4 selectivity of 21 and a CO_2/CH_4 selectivity of 4. Another interesting work from the same group is postsynthetic linker exchange of ZIF-8 with 2-imidazolecarboxaldehyde (Ica), which is the linker for ZIF-90.[132] ZIF-90 is isostructural with ZIF-8 but has a greater aperture size of 5.0 Å. By a controlled exchange with Ica, the selective ZIF-8 layer was still maintained while the exchanged top layer, composed of ZIF-90, reduced the resistance to propylene transport (Figure 11c,d). As a result, the propylene permeance increased by almost 4 times to 7.8 × 10^{-8} mol m^{-2}

DOI: 10.1021/acssuschemeng.8b05409
ACS Sustainable Chem. Eng. 2019, 7, 49−69

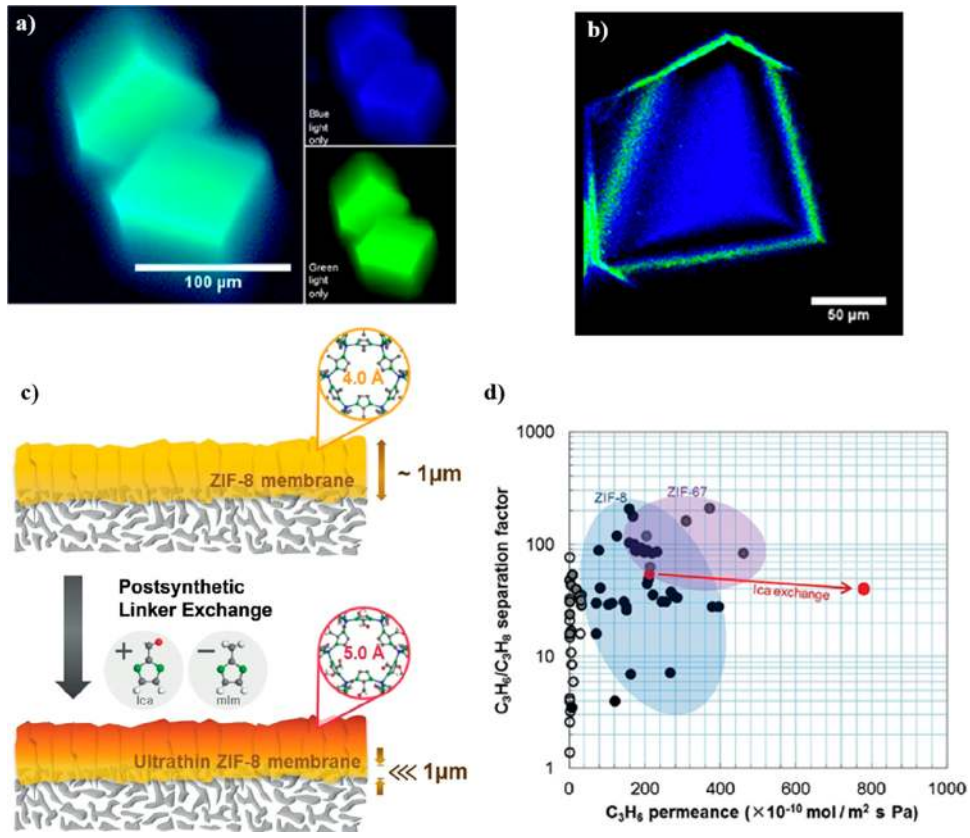

Figure 11. Confocal fluorescence microscopy image of ZIF-8−90 prepared by (a) de Novo synthesis and (b) solvent assisted linker exchange (SALE) method. While the de Novo synthesis leads to a unit cell mixing of the linker, SALE method results in a core−shell like structure. Reprinted with permission from reference 131. Copyright 2017 Americal Chemical Society. (c) Postsynthetic linker exchange of ZIF-8 membrane by Ica linker results in an effective decrease of the molecular selective layer because of the enlarged aperture upon Ica incorporation. (d) Increase in the propylene permeance as a result of reduced effective thickness of ZIF-8 membrane. Reprinted with permission from reference 132. Copyright 2018 John Wiley & Sons, Inc.

s^{-1} Pa while still retaining an impressive separation factor of 40.

Metal-Exchanged MOF Films. Compared to linker exchange, reports of metal exchange (also known as transmetalation) in MOF membranes are fewer in number. Li et al. reported the transformation of a HKUST-1 membrane to a hybrid HKUST-1/MIL-100 by immersing the membrane in a methanol based iron chloride solution.[133] The multivalent cation substitution process that produced the hybrid membrane, significantly improved the H_2/CO_2 and H_2/CH_4 selectivity by almost 1 order of magnitude to 89 and 336, respectively. They also demonstrated the feasibility of the method for the transformation of MOF-5 to HKUST-1 by Cu^{2+} substitution and further to MIL-53 by Fe^{3+} substitution. However, in this case, membrane results were not provided. Though not exactly a metal exchange process, Kwon et al. reported the heteroepitaxial growth of ZIF-67 (Co center) on ZIF-8 seed layer.[111] Compared to the Zn−N bond in ZIF-8, the Co−N bond in ZIF-67 was found to be stiffer, indicated by a blue shift of metal−N bond in FTIR. This restricted motion, leading to a slight decrease in the effective aperture size was pointed out as the reason for the observed very high propane/propylene separation factor of 85. Recently, the same group also reported a microwave assisted synthesis method for obtaining a mixed-metal (Co−Zn) ZIF-8 structure with a Co/Zn ratio of ∼1.[72] The resultant membrane exhibited almost a doubling of propane/propylene separation factor (∼120) while still maintaining a similar permeance (2.03×10^{-8} mol m^{-2} s^{-1} Pa^{-1}) compared to ZIF-8 membrane prepared under similar conditions.

MOF MEMBRANES FOR GAS SEPARATION

In the past decade, MOF membranes have been developed for several applications including gas separation, pervaporation, and desalination, demonstrating impressively high separation performance.[134−136] Here, we mainly focus on reports of polycrystalline MOF membranes from the past two years for propylene/propane, H_2/CO_2, CO_2/N_2 and CO_2/CH_4 separations. A summary of the performance of the MOF membranes for these separations will be presented using Robeson-like plots. There are several excellent reviews on the polycrystalline MOF membranes for gas separation prior to 2016.[19−21,24,42,137]

Propylene/Propane Separation. Propylene/propane separation, currently accomplished by energy-intensive cryogenic distillation, is quite challenging yet commercially important due to the close physical properties. A typically quoted performance target for this separation is propylene permeance higher than 3.3×10^{-8} mol m^{-2} s^{-1} Pa^{-1} and separation factor higher than 30.[111] Employing process simulations, Tsapatsis and co-workers recently demonstrated that compared to the standalone distillation, a hybrid membrane/distillation process can increase the productivity by 35%.[10] A permeance of 100 GPU and separation factor of

DOI: 10.1021/acssuschemeng.8b05409
ACS Sustainable Chem. Eng. 2019, 7, 49−69

50 with feed pressure of 7 bar and permeate pressure of 1 bar was considered for above calculation. MOF, in particular, ZIF-8 has been extensively investigated for this separation. Although the pore aperture of ZIF-8 is 3.4 Å, the effective pore aperture is around 4 Å owing to the lattice flexibility.[134] The diffusivity of propylene in ZIF-8 is 2 orders of magnitude higher than that of propane, indicating that ZIF-8 membrane can effectively separate propylene from propane. Overall, from the documented ZIF-8 membranes for propylene/propane separation, we can find that the key to high selectivity is that the MOF membrane should be of high quality and nearly defect-free. Lai and co-workers reported the first ZIF-8 membrane by a seeded secondary growth method for propylene/propane separation in 2012, exhibiting a propylene permeance of 2.8×10^{-8} mol m^{-2} s^{-1} Pa^{-1} with a separation factor of 35.[73] Jeong and co-workers reported a ZIF-8 membrane with a higher quality using an *in situ* method in 2013, exhibiting a propylene permeance of 2.1×10^{-8} mol m^{-2} s^{-1} Pa^{-1} with a separation factor of 50.[134] Since then, the interest in MOF membrane for propylene/propane separation has ignited. Most of the high-performance MOF membranes are based on ZIF-8 and related hybrids (Figure 12).

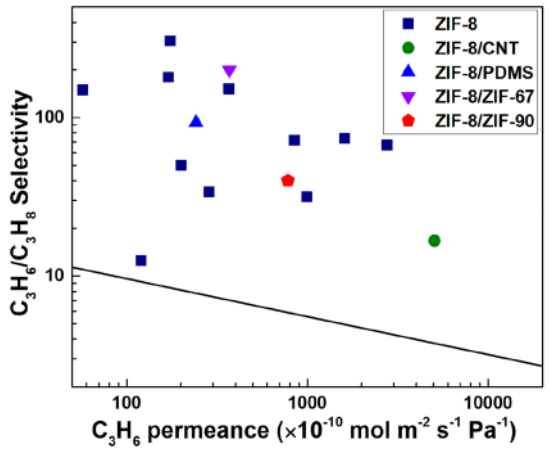

Figure 12. Comparison of propylene/propane separation performance of the documented MOF membranes: ZIF-8,[10,44,45,48,50,51,73,113,134] ZIF-8/CNT,[62] ZIF-8/PDMS,[138] ZIF-8/ZIF-67,[111] ZIF-8/ZIF-90.[132] The black line represents the propylene/propane upper bound limit for polymeric membranes.[139]

Approaches to increase the propylene/propane selectivity typically involve reducing the defects in the membrane or shrinking the effective aperture size of ZIF frameworks. Kwon et al. reported a 700 nm-thick ZIF-67 membrane by heteroepitaxially growing ZIF-67 on ZIF-8 seed layer, exhibiting a propylene permeance of 4.6×10^{-8} mol m^{-2} s^{-1} Pa^{-1} with a propylene/propane separation factor of ~85.[111] The high selectivity may stem from the slightly smaller effective pore aperture of ZIF-67, attributing to the fact the Co−N bonds are more rigid than the Zn−N bonds. Furthermore, a tertiary heteroepitaxial growth of ZIF-8 layers on ZIF-67 membranes leads to a remarkable increase in propylene/propane separation factor to 200, possibly due to the improved grain-boundary structure. Wang et al. reported a different separation behavior; that is, pure ZIF-67 membrane only showed a propylene/propane separation factor of 1.4, which increased to 50.5 when 90% Co in ZIF-67 was replaced by Zn.[140] The authors found that the diffusion of propane in the Zn-substituted ZIF-67 crystals become slower with the increase of the zinc content, implying that incorporation of Zn^{2+} into the ZIF-67 could decrease the effective pore aperture of the framework. Considering the different explanation in the effective pore aperture of ZIF-67, more studies need to be undertaken to reveal the difference between ZIF-8 and ZIF-67 membrane in microstructure and transport phenomenon. Barankova et al. prepared a 620 nm-thick ZIF-8 membrane on a metal-chelating polymer support via a one-step contra-diffusion crystallization method.[48] It was found that the propylene/propane ideal selectivity increased from 22 to 150, after sealing the defects in the interface by coating a thin layer of poly[1-(trimethylsilyl)-1-propyne] (PTMSP). The membrane showed a high H_2/C_3H_8 ideal selectivity over 8000, indicating the nearly defect-free feature. Sheng et al. also found a similar behavior: they coated a ZIF-8 membrane with polydimethylsiloxane (PDMS) and observed a significant enhancement in the propylene/propane separation factor, from 46 to 104 in one case, and from 3 to 54 in another case.[138] They hypothesized that the PDMS blocked the intercrystalline defects as well as hindered the flexibility of the ZIF-8 framework. The polymer coating can also improve the hydrolytic stability and pressure stability of ZIF-8 membranes. The recently reported fast current drive synthesis method by Zhou et al. produced a ZIF-8 membrane with suppressed linker mobility by an electrochemical method and demonstrated an impressive propylene/propane separation factor of 304.8 with a propylene permeance of 1.7×10^{-8} mol m^{-2} s^{-1} Pa^{-1}.[113] The direct current promotes the metal ions and ligands to assemble into inborn-distorted and stiffer frameworks, accounting for the ultrahigh selectivity.

Another important direction for propylene/propane separation is to increase the propylene permeance, which is usually achieved by decreasing the membrane thickness to an ultrathin scale (sub-500 nm). Recently, our group reported an ENACT approach for the synthesis of a 500 nm-thick ZIF-8 membrane on an unmodified AAO.[51] Thanks to the ultrathin and nearly defect-free features, the ENACT-derived ZIF-8 membrane showed a high C_3H_6 permeance of 9.9×10^{-8} mol m^{-2} s^{-1} Pa^{-1} with a C_3H_6/C_3H_8 selectivity of 31.6. Lee et al. reported a linker exchange of 2-methylimidazole in ZIF-8 membrane with 2-imidazolecarboxaldehyde (ZIF-90 linker, Figure 11c,d), leading to the increase of the effective aperture size of ZIF-8 and reduction of the effective membrane thickness.[132] As a result, the linker-exchanged ZIF-8 membrane exhibited a 4-fold increase in the propylene permeance, reaching up to 7.8×10^{-8} mol m^{-2} s^{-1} Pa^{-1}, with only a slight decrease in the propylene/propane separation factor.

H_2/CO_2 Separation. Currently, over 96% of the H_2 is produced by the reforming of fossil-fuel, which necessitates a H_2/CO_2 separation process. Current commercial separation technology mainly relies on the amine-based CO_2 scrubbing. However, the high cost of amine regeneration, as well as the environmental concerns on the amine loss into atmosphere, have motivated researchers to develop an energy-efficient alternative. Not surprisingly, the membrane-processes can play a key role here. One of the most promising membranes for this separation is dense metal film, mainly those based on Pd. However, the high cost as well as the chemical stability issues of these membranes have so far prevented their implementation. MOFs provide a unique opportunity for this separation, where an efficient separation of H_2 from CO_2 can be carried

DOI: 10.1021/acssuschemeng.8b05409
ACS Sustainable Chem. Eng. 2019, 7, 49−69

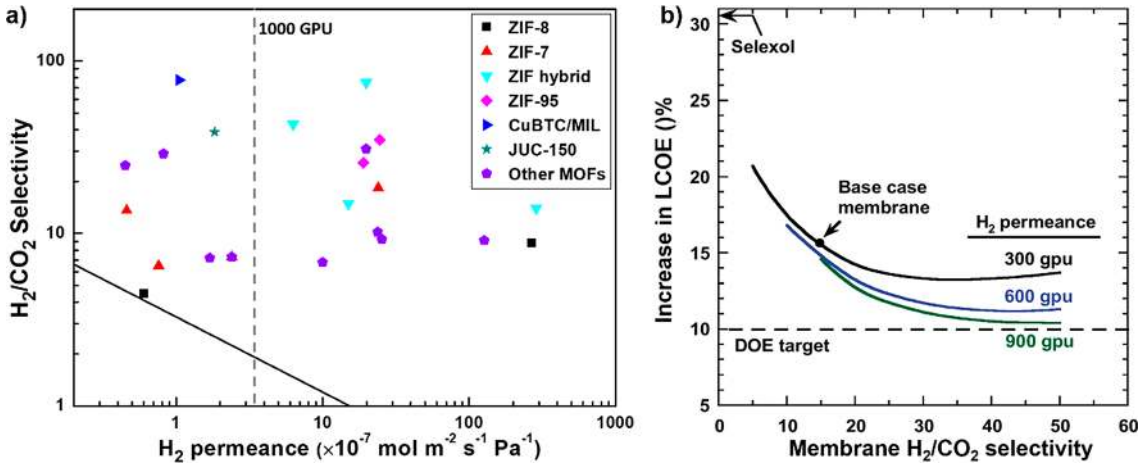

Figure 13. (a) Comparison of H_2/CO_2 separation performance of the different MOF membranes: ZIF-8,[39,146] ZIF-7,[56,58,147,148] ZIF hybrid,[62,64,114,149] ZIF-95,[142] CuBTC/MIL,[133] JUC-150[143] and other MOFs.[66,97,143,144,150−154] The black line represents the H_2/CO_2 upper bound limit for polymeric membranes. (b) Increase in levelized cost of the electricity (LCOE) resulting from changes in membrane properties at 90% CO_2 capture. Reprinted with permission from reference 145. Copyright 2012 Elsevier.

out by size-sieving. To achieve this, the selected MOFs should possess aperture between the kinetic diameters of H_2 (2.9 Å) and CO_2 (3.3 Å) if the lattice is rigid or should have an aperture below 2.9 Å if the lattice is flexible. Up to now, the MOF membranes that shows H_2/CO_2 selectivity higher than 10 include ZIF-7,[56] ZIF-8,[39] ZIF-9,[141] ZIF-95,[142] CuBTC/MIL-100,[133] JUC-150,[143] NH_2-MIL-53[144] and NH_2-MIL-125(Ti)[97] based membranes (Figure 13a). Most of the MOF membranes that have demonstrated a good H_2/CO_2 separation performance, transcend the Robeson-like upper bound line because of the inherent high porosity of MOFs (Figure 13a). However, MOF membranes showing a H_2/CO_2 selectivity higher than 30 are few mainly due to the absence of rigid MOFs with pore aperture that lies between the diameter of these two gas pairs. To meet the US DOE target, the MOF membranes should have a CO_2 permeance higher than 3.3×10^{-7} mol m^{-2} s^{-1} Pa^{-1}, and a H_2/CO_2 separation factor in the range of 30−50 (Figure 13b).[145] Below, we discuss a few MOF structures that have been studied for this separation.

The rhombohedral phase of ZIF-7 has an aperture size of ∼3 Å and has a high thermal stability (up to 500 °C), making it a promising candidate material for H_2/CO_2 separation. However, the synthesis of a highly selective, defect-free ZIF-7 membrane remains a big challenge mainly because DMF is both the solvent and template for the rhombohedral phase of ZIF-7. Removal of DMF from ZIF-7 is accompanied by a phase change in ZIF-7.[116] Until now, the H_2/CO_2 separation factors from the reported ZIF-7 membrane are below 20. The first selective ZIF-7 membrane (2 μm thick) on alumina disc was demonstrated by Caro and co-workers in 2010, which shows a H_2/CO_2 separation factor of 13.6 and a H_2 permeance of 4.6×10^{-8} mol m^{-2} s^{-1} Pa^{-1} at 220 °C.[56,58] However, the crystal structure of the activated membrane was not reported. Li et al. reported the synthesis of ZIF-7 membrane by growing the ZIF-7 film on a ZnO-array modified PVDF hollow fiber in a ZIF-7 precursor.[148] The resulting 10 μm-thick ZIF-7 membrane showed a H_2 permeance of 2.4×10^{-6} mol m^{-2} s^{-1} Pa^{-1} with a H_2/CO_2 ideal separation factor of 18.4 at 25 °C. It is noteworthy that the permeability of this ZIF-7 membrane is at least 260 times higher than that of the ZIF-7 reported by Caro and co-workers, implying that the ZIF-7 microstructures from different synthesis methods are different.

ZIF-8 membrane can also be used for H_2/CO_2 separation when the ZIF-8 lattice flexibility is hindered. This can be achieved by combining ZIF-8 with other nanoporous materials such as CNT or GO nanoporous films, which are postulated to make ZIF-8 lattice more rigid. Shamsaei et al. prepared ZIF-8/CNT hybrid membrane by depositing a dopamine-modified CNT film on a porous substrate, followed by the contra-diffusion based crystallization.[62] The resulting 200 nm-thick ZIF-8/CNT membrane showed an ultrahigh H_2 permeance of 2.9×10^{-5} mol m^{-2} s^{-1} Pa^{-1} with a H_2/CO_2 ideal selectivity of 14. Zhang et al. reported a 550 nm-thick ZIF-8/CNT membrane by a similar contra-diffusion method using a dopamine-modified CNT film as a support.[64] However, the transport behavior is completely different from the previous ZIF-8/CNT membrane. This ZIF-8/CNT membrane showed a H_2 permeance of 6.3×10^{-7} mol m^{-2} s^{-1} Pa^{-1} with a H_2/CO_2 ideal separation factor of 43, implying a more rigid ZIF-8 lattice. Kang et al. reported the synthesis of a 500 nm-thick ZIF-67/GO membrane by a two-dimensional confinement strategy; that is, converting $Co(OH)_2$/GO precursors to a ZIF-67/GO membrane.[149] The ZIF-67/GO membrane demonstrated a H_2 permeance of 2.0×10^{-6} mol m^{-2} s^{-1} Pa^{-1} with a high H_2/CO_2 separation factor of 75 at 25 °C. Because the synthesis of ZIF-8 membrane is much easier and more straightforward compared with many other MOF membranes, a rational way to achieve MOF membrane for H_2/CO_2 separation could be engineering the lattice flexibility of ZIF-8 membrane.

Sun et al. reported the synthesis of *c*-oriented NH_2-MIL-125(Ti) (aperture size: 5−6 Å) membranes on α-Al_2O_3 support by combining oriented seeding and controlled in-plane epitaxial growth, demonstrating an ideal H_2/CO_2 selectivity of 24.8, 6-fold higher than their randomly oriented counterparts.[97] The optimized *c*-oriented membrane showed a H_2 permeance of 4.5×10^{-8} mol m^{-2} s^{-1} Pa^{-1} with an ideal selectivity of 24.8 (H_2/CO_2), 10.4 (H_2/N_2) and 11.4 (H_2/CH_4). Although this MOF has a straight channel along the *c*-axis and the membrane thickness was only 500 nm, the H_2 permeance is unexpectedly low, possibly due to a partial blockage of MOF channels. Zhang et al. reported the synthesis

DOI: 10.1021/acssuschemeng.8b05409
ACS Sustainable Chem. Eng. 2019, 7, 49−69

of 15 μm-thick NH_2-MIL-53(Al) (aperture size 7.5 Å) membrane by a conventional seeded secondary growth method.[144] This much thicker membrane showed a significantly high H_2 permeance of 2.7×10^{-6} mol m^{-2} s^{-1} Pa^{-1} with an ideal selectivity of 27.3 (H_2/CO_2), 19.5 (H_2/N_2) and 18.5 (H_2/CH_4). Interestingly, both the *c*-oriented NH_2-MIL-125(Ti) and the NH_2-MIL-53(Al) showed higher H_2/CO_2 selectivity compared to that of H_2/CH_4. This can be attributed to the high sorption affinity of the amino-based MOFs toward CO_2, which suppresses the diffusion of CO_2. These two studies suggest that MOFs with pore aperture larger than 4 Å can also be employed for an efficient H_2/CO_2 separation by taking advantage of the competitive mixture adsorption effect rather than the size-sieving.

CO_2/N_2 and CO_2/CH_4 Separation. The development of MOF membranes for the separation of CO_2/N_2 and CO_2/CH_4 is essential for the carbon capture and the purification/sweetening of biogas and natural gas. A typical performance target for such separation requires a CO_2 permeance higher than 3.3×10^{-7} mol m^{-2} s^{-1} Pa^{-1}, and a mixture separation factor of at least 20.[155] MOF structures that can separate these gas pairs by size-sieving are scarce mainly because of the fact that the kinetic diameters of these gas pairs are extremely close and there is a lack of rigid MOFs that have an effective aperture in the range of 3.3−3.8 Å, which can be processed into a high-quality polycrystalline film. Up to now, the MOF membranes that have shown a high CO_2 permselectivity include CAU-1[156,157] and MOF-5,[158] which were developed by Lin and co-workers.

CAU-1, also referred to as $Al_4(OH)_2(OCH_3)_4(H_2N\text{-}BDC)_3$, has an aperture size of 3−4 Å and exhibits high porosity, good thermal/chemical stability, and high CO_2 adsorption capacity, which makes it highly promising for CO_2 separation. Yin et al. reported the synthesis of a 2−3 μm-thick CAU-1 membrane on an alumina tube for CO_2/N_2 mixture separation by a seeded secondary growth method. The CO_2 permeance was 5.7×10^{-7} mol m^{-2} s^{-1} Pa^{-1} with a corresponding CO_2/N_2 separation factor of 17.4.[156] The high adsorption uptake of CO_2 in the CAU-1 facilitated by the strong acid−base interactions between CO_2 and the amino groups, played a key role in promoting the CO_2 permeance and selectivity.

Rui et al. reported the "sharp molecular sieving" properties of a 14 μm-thick MOF-5 membrane, prepared by a secondary growth method, for CO_2 separation from a dry CO_2 enriched (>80%) CO_2/CH_4 and CO_2/N_2 mixtures.[158] The membrane demonstrated CO_2/CH_4 and CO_2/N_2 separation factors of 328 and 410, respectively, with the CO_2 permeance of $2.1-2.6 \times 10^{-7}$ mol m^{-2} s^{-1} Pa^{-1}. The pore aperture of MOF-5 is around 12 Å,[159] implying that the high selectivity is not provided by the size-cutoff mechanism. Thus, this high selectivity is attributed to the exceptionally high CO_2 uptake of MOF-5, benefiting the CO_2 adsorption-driven selectivity. It should be noted that MOF-5 is not stable in humidified conditions. This study suggests that the MOF membranes with CO_2-phillic functional group can be employed for CO_2 separation even when the aperture size is larger than the kinetic diameter of N_2 or CH_4. This concept can extend the library of MOFs used for the CO_2 separation.

SUMMARY

We have discussed several crystal engineering approaches that were successful in controlling the morphology of polycrystalline MOF films and reducing/managing lattice flexibility and defects. In a relatively short period, these approaches have elevated MOF-films as the state-of-the-art nanoporous membranes for gas separation, making MOF-based membranes highly promising to substitute or supplement energy-intensive gas separations, especially C_3H_6/C_3H_8 and H_2/CO_2. Still, there are many opportunities for further improvement in performance and challenges for the potential scale-up of the polycrystalline MOF membranes. Further development of characterization techniques, especially microscopy, to observe defects such as grain-boundary defects will greatly help to understand and alleviate the role of defects in molecular separation. Also, there are several MOF structures, deemed nonporous by the classical N_2-adsorption based porosity studies, that could be interesting for the sieving of He and H_2 from the larger molecules such as CO_2 and CH_4. An example of this is the monoclinic phase of ZIF-7, also known as the phase III of ZIF-7.[116] These typically have a crystallographically determined pore-aperture of 0.21 nm, yet, Peng et al. were able to exploit these pores for sieving H_2 from CO_2, benefiting from the lattice flexibility of ZIF-7.[160] In this respect, fresh screening of the database of MOFs with an eye on the structures possessing small-pores could yield several high-performance candidates for the gas sieving. There is also a large opportunity space for restricting lattice flexibility of MOFs with pore-size in the range of 0.30−0.34 nm, such as ZIF-8, for sieving CO_2 from N_2 and CH_4.

One of the most important challenges for nanoporous membranes is their efficient scale-up to meet the capacity to tackle industrial-scale separations. MOFs have emerged to be the most promising nanoporous membranes; however, most of the performance demonstration has been carried out on centimeter-sized disks. The hollow-fiber based modules offer a high surface area to volume ratio, and therefore MOF membranes based on hollow-fiber supports are highly desirable. The key challenge is the brittleness of the MOF structure. Although MOFs are coordination polymers, their crystalline lattice makes MOF films highly prone to develop cracks on flexible substrates. As a result, the synthesis of MOF films on a highly flexible porous substrate such as hollow-fiber is always tricky. Although there are several reports of successful crystallization of high-performance MOF films on hollow-fiber supports, most of these films were fabricated with a great care on a single hollow-fiber strand or an already assembled hollow-fiber support module. The performance of the latter is usually lower than the single hollow-fiber membranes. Therefore, the research community is motivated to develop novel strategies that will yield MOF films resistant to mechanical failure. In this respect, a strategy is to develop mixed matrix membranes, combining the processability of polymers with the separation performance of MOFs. Another actively pursued strategy is a generic synthesis route to MOF nanosheets, allowing the fabrication of MOF thin films by simple coating processes. The mechanical stability of such films is a subject of investigation. Another strategy is the reduction of film thickness, to the scale of a few nanometers, reducing the bending-related strain in the film. Progress in these aspects will accelerate the adaptation of MOF membranes in the chemical industry.

AUTHOR INFORMATION

Corresponding Author

*K. V. Agrawal. E-mail: kumar.agrawal@epfl.ch.

DOI: 10.1021/acssuschemeng.8b05409
ACS Sustainable Chem. Eng. 2019, 7, 49−69

ORCID

Luis Francisco Villalobos: 0000-0002-0745-4246
Kumar Varoon Agrawal: 0000-0002-5170-6412

Author Contributions

†These authors contributed equally.

Notes

The authors declare no competing financial interest.

Biographies

Deepu J. Babu is a postdoc at the Laboratory of Advanced Separations (LAS) at École Polytechnique Fédérale de Lausanne (EPFL). He obtained his Master's degree in Materials Engineering in 2011 from the Indian Institute of Technology (IIT) Madras, Chennai. He joined the research group of Prof. Jörg J. Schneider at TU Darmstadt and earned his Dr.rer.nat. degree in 2016 investigating the gas adsorption characteristics of aligned carbon nanotubes. Since 2017, he is a postdoc in Prof. K. V. Agrawal's research group and his current research focuses on inorganic membranes for gas separation.

Guangwei He is a postdoc at the laboratory of advanced separations (LAS) at École Polytechnique Fédérale de Lausanne (EPFL). He received his Ph.D. in Chemical Engineering from Tianjin University under the guidance of Prof. Zhongyi Jiang and Prof. Michael D. Guiver, where he worked on advanced ion conducting membranes. At EPFL, he studies the engineering of MOF membranes and nanoporous graphene membranes with Prof. Kumar Varoon Agrawal. His research interest focuses on nanomaterials-based inorganic membranes and composite membranes for gas separation and ion conduction.

Luis Francisco Villalobos is a postdoc at the Laboratory of Advanced Separations (LAS) at École Polytechnique Fédérale de Lausanne (EPFL). He received his Ph.D. in Chemical Engineering from King Abdullah University of Science and Technology (KAUST) working with Prof. Klaus-Viktor Peinemann, where he developed strategies to use intrinsically porous molecules as the main building block for membranes and pioneered the development of a phase inversion technique to concentrate metal ions in only the selective layer of polymeric membranes for applications like hydrogen recovery, biofouling control, and catalysis. At EPFL, he focuses on developing approaches for the fabrication of two-dimensional nanoporous membranes and studying how molecules transport across them.

Kumar Varoon Agrawal is an assistant professor at the Institute of Chemical Sciences and Engineering (ISIC) at École Polytechnique Fédérale de Lausanne (EPFL) where he heads the Laboratory of Advanced Separations (LAS). He received his Ph.D. in Chemical Engineering from the University of Minnesota working with Prof. Michael Tsapatsis and Prof. Lorraine Francis where he developed the two-dimensional zeolite nanosheets. In his postdoctoral research with Prof. Michael Strano at the Massachusetts Institute of Technology, he studied the effect of nanoconfinement on the phase transition of fluids. He started his research group at EPFL in 2016 focusing on developing synthetic routes for the two-dimensional nanoporous membranes with a precise control of nanopore size and functionality. His awards include University of Minnesota Doctoral Degree Fellowship, AIChE Separations Division Graduate Student Research Award, and North American Membrane Society Young Membrane Scientist Award.

■ ACKNOWLEDGMENTS

We acknowledge our host institute, EPFL, for financial support. A part of the work was funded by the Swiss National Science Foundation, AP Energy Grant, grant no.

DOI: 10.1021/acssuschemeng.8b05409
ACS Sustainable Chem. Eng. 2019, 7, 49−69

PYAPP2_173645. Authors acknowledge the financial support from the Swiss Competence Center of Energy Research – Efficiency in Industrial Process, grant no. 1155002538. G.H. acknowledges support from the EPFL Fellows program, which received funding from the Horizon 2020 Research and innovation program under the Marie Skłodowska-Curie grant agreement no. 665667.

REFERENCES

(1) Humphrey, J. L.; Keller, G. E. *Separation Process Technology*; Builders' Guides; McGraw-Hill, 1997.
(2) Robeson, L. M. Correlation of Separation Factor versus Permeability for Polymeric Membranes. *J. Membr. Sci.* **1991**, *62* (2), 165–185.
(3) Robeson, L. M. The Upper Bound Revisited. *J. Membr. Sci.* **2008**, *320* (1), 390–400.
(4) Park, H. B.; Jung, C. H.; Lee, Y. M.; Hill, A. J.; Pas, S. J.; Mudie, S. T.; Van Wagner, E.; Freeman, B. D.; Cookson, D. J. Polymers with Cavities Tuned for Fast Selective Transport of Small Molecules and Ions. *Science* **2007**, *318* (5848), 254–258.
(5) Budd, P. M.; McKeown, N. B.; Fritsch, D. Free Volume and Intrinsic Microporosity in Polymers. *J. Mater. Chem.* **2005**, *15* (20), 1977–1986.
(6) Park, H. B.; Kamcev, J.; Robeson, L. M.; Elimelech, M.; Freeman, B. D. Maximizing the Right Stuff: The Trade-off between Membrane Permeability and Selectivity. *Science* **2017**, *356* (6343), eaab0530.
(7) Furukawa, H.; Cordova, K. E.; O'Keeffe, M.; Yaghi, O. M. The Chemistry and Applications of Metal-Organic Frameworks. *Science* **2013**, *341* (6149), 1230444.
(8) Peng, Y.; Krungleviciute, V.; Eryazici, I.; Hupp, J. T.; Farha, O. K.; Yildirim, T. Methane Storage in Metal–Organic Frameworks: Current Records, Surprise Findings, and Challenges. *J. Am. Chem. Soc.* **2013**, *135* (32), 11887–11894.
(9) McDonald, T. M.; Mason, J. A.; Kong, X.; Bloch, E. D.; Gygi, D.; Dani, A.; Crocellà, V.; Giordanino, F.; Odoh, S. O.; Drisdell, W. S.; et al. Cooperative Insertion of CO2 in Diamine-Appended Metal-Organic Frameworks. *Nature* **2015**, *519*, 303.
(10) Ma, X.; Kumar, P.; Mittal, N.; Khlyustova, A.; Daoutidis, P.; Mkhoyan, K. A. A.; Tsapatsis, M. Zeolitic Imidazolate Framework Membranes Made by Ligand-Induced Permselectivation. *Science* **2018**, *361* (6406), 1008–1011.
(11) Santos, V. P.; Wezendonk, T. A.; Jaén, J. J. D.; Dugulan, A. I.; Nasalevich, M. A.; Islam, H.-U.; Chojecki, A.; Sartipi, S.; Sun, X.; Hakeem, A. A.; et al. Metal Organic Framework-Mediated Synthesis of Highly Active and Stable Fischer–Tropsch Catalysts. *Nat. Commun.* **2015**, *6*, 6451.
(12) Zhu, L.; Liu, X.-Q.; Jiang, H.-L.; Sun, L.-B. Metal–Organic Frameworks for Heterogeneous Basic Catalysis. *Chem. Rev.* **2017**, *117* (12), 8129–8176.
(13) Wang, H.; Zhu, Q.-L.; Zou, R.; Xu, Q. Metal-Organic Frameworks for Energy Applications. *Chem.* **2017**, *2* (1), 52–80.
(14) Chaikittisilp, W.; Hu, M.; Wang, H.; Huang, H.-S.; Fujita, T.; Wu, K. C.-W.; Chen, L.-C.; Yamauchi, Y.; Ariga, K. Nanoporous Carbons through Direct Carbonization of a Zeolitic Imidazolate Framework for Supercapacitor Electrodes. *Chem. Commun.* **2012**, *48* (58), 7259–7261.
(15) Stavila, V.; Talin, A. A.; Allendorf, M. D. MOF-Based Electronic and Opto-Electronic Devices. *Chem. Soc. Rev.* **2014**, *43* (16), 5994–6010.
(16) Gu, Z.-G.; Chen, S.-C.; Fu, W.-Q.; Zheng, Q.; Zhang, J. Epitaxial Growth of MOF Thin Film for Modifying the Dielectric Layer in Organic Field-Effect Transistors. *ACS Appl. Mater. Interfaces* **2017**, *9* (8), 7259–7264.
(17) Wilmer, C. E.; Leaf, M.; Lee, C. Y.; Farha, O. K.; Hauser, B. G.; Hupp, J. T.; Snurr, R. Q. Large-Scale Screening of Hypothetical Metal–organic Frameworks. *Nat. Chem.* **2012**, *4*, 83.
(18) Martin, R. L.; Lin, L.-C.; Jariwala, K.; Smit, B.; Haranczyk, M. Mail-Order Metal–Organic Frameworks (MOFs): Designing Isoreticular MOF-5 Analogues Comprising Commercially Available Organic Molecules. *J. Phys. Chem. C* **2013**, *117* (23), 12159–12167.
(19) Shah, M.; McCarthy, M. C.; Sachdeva, S.; Lee, A. K.; Jeong, H.-K. Current Status of Metal–Organic Framework Membranes for Gas Separations: Promises and Challenges. *Ind. Eng. Chem. Res.* **2012**, *51* (5), 2179–2199.
(20) Qiu, S.; Xue, M.; Zhu, G. Metal-Organic Framework Membranes: From Synthesis to Separation Application. *Chem. Soc. Rev.* **2014**, *43* (16), 6116–6140.
(21) Adatoz, E.; Avci, A. K.; Keskin, S. Opportunities and Challenges of MOF-Based Membranes in Gas Separations. *Sep. Purif. Technol.* **2015**, *152*, 207–237.
(22) Adil, K.; Belmabkhout, Y.; Pillai, R. S.; Cadiau, A.; Bhatt, P. M.; Assen, A. H.; Maurin, G.; Eddaoudi, M. Gas/vapour Separation Using Ultra-Microporous Metal–organic Frameworks: Insights into the Structure/separation Relationship. *Chem. Soc. Rev.* **2017**, *46* (11), 3402–3430.
(23) Zhao, X.; Wang, Y.; Li, D.-S.; Bu, X.; Feng, P. Metal–Organic Frameworks for Separation. *Adv. Mater.* **2018**, *30* (37), 1705189.
(24) Rangnekar, N.; Mittal, N.; Elyassi, B.; Caro, J.; Tsapatsis, M. Zeolite Membranes – a Review and Comparison with MOFs. *Chem. Soc. Rev.* **2015**, *44* (20), 7128–7154.
(25) Davis, T. M.; Drews, T. O.; Ramanan, H.; He, C.; Dong, J.; Schnablegger, H.; Katsoulakis, M. A.; Kokkoli, E.; McCormick, A. V.; Penn, R. L.; et al. Mechanistic Principles of Nanoparticle Evolution to Zeolite Crystals. *Nat. Mater.* **2006**, *5*, 400.
(26) Lupulescu, A. I.; Rimer, J. D. In Situ Imaging of Silicalite-1 Surface Growth Reveals the Mechanism of Crystallization. *Science* **2014**, *344* (6185), 729–732.
(27) Aerts, A.; Haouas, M.; Caremans, T. P.; Follens, L. R. A.; van Erp, T. S.; Taulelle, F.; Vermant, J.; Martens, J. A.; Kirschhock, C. E. A. Investigation of the Mechanism of Colloidal Silicalite-1 Crystallization by Using DLS, SAXS, and 29Si NMR Spectroscopy. *Chem. - Eur. J.* **2010**, *16* (9), 2764–2774.
(28) Cravillon, J.; Schröder, C. A.; Nayuk, R.; Gummel, J.; Huber, K.; Wiebcke, M. Fast Nucleation and Growth of ZIF-8 Nanocrystals Monitored by Time-Resolved In Situ Small-Angle and Wide-Angle X-Ray Scattering. *Angew. Chem., Int. Ed.* **2011**, *50* (35), 8067–8071.
(29) Venna, S. R.; Jasinski, J. B.; Carreon, M. A. Structural Evolution of Zeolitic Imidazolate Framework-8. *J. Am. Chem. Soc.* **2010**, *132* (51), 18030–18033.
(30) Van Vleet, M. J.; Weng, T.; Li, X.; Schmidt, J. R. R. In Situ, Time-Resolved, and Mechanistic Studies of Metal–Organic Framework Nucleation and Growth. *Chem. Rev.* **2018**, *118* (7), 3681–3721.
(31) Demazeau, G. Solvothermal Reactions: An Original Route for the Synthesis of Novel Materials. *J. Mater. Sci.* **2008**, *43* (7), 2104–2114.
(32) Avrami, M. Kinetics of Phase Change. I General Theory. *J. Chem. Phys.* **1939**, *7* (12), 1103–1112.
(33) Gualtieri, A. F. Synthesis of Sodium Zeolites from a Natural Halloysite. *Phys. Chem. Miner.* **2001**, *28* (10), 719–728.
(34) Seoane, B.; Zamaro, J. M.; Tellez, C.; Coronas, J. Sonocrystallization of Zeolitic Imidazolate Frameworks (ZIF-7, ZIF-8, ZIF-11 and ZIF-20). *CrystEngComm* **2012**, *14* (9), 3103–3107.
(35) Cravillon, J.; Münzer, S.; Lohmeier, S.-J.; Feldhoff, A.; Huber, K.; Wiebcke, M. Rapid Room-Temperature Synthesis and Characterization of Nanocrystals of a Prototypical Zeolitic Imidazolate Framework. *Chem. Mater.* **2009**, *21* (8), 1410–1412.
(36) Yao, J.; Dong, D.; Li, D.; He, L.; Xu, G.; Wang, H. Contra-Diffusion Synthesis of ZIF-8 Films on a Polymer Substrate. *Chem. Commun.* **2011**, *47* (9), 2559–2561.
(37) Öztürk, Z.; Filez, M.; Weckhuysen, B. M. Decoding Nucleation and Growth of Zeolitic Imidazolate Framework Thin Films with Atomic Force Microscopy and Vibrational Spectroscopy. *Chem. - Eur. J.* **2017**, *23* (45), 10915–10924.

DOI: 10.1021/acssuschemeng.8b05409
ACS Sustainable Chem. Eng. 2019, 7, 49–69

(38) Park, K. S.; Ni, Z.; Cote, A. P.; Choi, J. Y.; Huang, R.; Uribe-Romo, F. J.; Chae, H. K.; O'Keeffe, M.; Yaghi, O. M. Exceptional Chemical and Thermal Stability of Zeolitic Imidazolate Frameworks. *Proc. Natl. Acad. Sci. U. S. A.* **2006**, *103* (27), 10186−10191.
(39) Bux, H.; Liang, F.; Li, Y.; Cravillon, J.; Wiebcke, M.; Caro, J. J. Zeolitic Imidazolate Framework Membrane with Molecular Sieving Properties by Microwave-Assisted Solvothermal Synthesis. *J. Am. Chem. Soc.* **2009**, *131* (44), 16000−16001.
(40) Shah, M.; Kwon, H. T.; Tran, V.; Sachdeva, S.; Jeong, H.-K. One Step in Situ Synthesis of Supported Zeolitic Imidazolate Framework ZIF-8 Membranes: Role of Sodium Formate. *Microporous Mesoporous Mater.* **2013**, *165*, 63−69.
(41) Pan, Y.; Liu, Y.; Zeng, G.; Zhao, L.; Lai, Z. Rapid Synthesis of Zeolitic Imidazolate Framework-8 (ZIF-8) Nanocrystals in an Aqueous System. *Chem. Commun.* **2011**, *47* (7), 2071−2073.
(42) Yao, J.; Wang, H. Zeolitic Imidazolate Framework Composite Membranes and Thin Films: Synthesis and Applications. *Chem. Soc. Rev.* **2014**, *43* (13), 4470−4493.
(43) Kang, Z.; Fan, L.; Sun, D. Recent Advances and Challenges of Metal-Organic Framework Membranes for Gas Separation. *J. Mater. Chem. A* **2017**, *5* (21), 10073−10091.
(44) Brown, A. J. A. J.; Brunelli, N. A. N. A.; Eum, K.; Rashidi, F.; Johnson, J. R. R.; Koros, W. J. W. J.; Jones, C. W. C. W.; Nair, S. Interfacial Microfluidic Processing of Metal-Organic Framework Hollow Fiber Membranes. *Science* **2014**, *345* (6192), 72−75.
(45) Eum, K.; Ma, C.; Rownaghi, A.; Jones, C. W.; Nair, S. ZIF-8 Membranes via Interfacial Microfluidic Processing in Polymeric Hollow Fibers: Efficient Propylene Separation at Elevated Pressures. *ACS Appl. Mater. Interfaces* **2016**, *8* (38), 25337−25342.
(46) Huang, K.; Wang, B.; Chi, Y.; Li, K. High Propylene Selective Metal-Organic Framework Membranes Prepared in Confined Spaces via Convective Circulation Synthesis. *Adv. Mater. Interfaces* **2018**, *5* (18), 1800287.
(47) Liang, K.; Ricco, R.; Doherty, C. M.; Styles, M. J.; Bell, S.; Kirby, N.; Mudie, S.; Haylock, D.; Hill, A. J.; Doonan, C. J.; et al. Biomimetic Mineralization of Metal-Organic Frameworks as Protective Coatings for Biomacromolecules. *Nat. Commun.* **2015**, *6*, 1−8.
(48) Barankova, E.; Tan, X.; Villalobos, L. F.; Litwiller, E.; Peinemann, K.-V. V. A Metal Chelating Porous Polymeric Support: The Missing Link for a Defect-Free Metal−organic Framework Composite Membrane. *Angew. Chem., Int. Ed.* **2017**, *56* (11), 2965−2968.
(49) Hou, J.; Sutrisna, P. D.; Zhang, Y.; Chen, V. Formation of Ultrathin, Continuous Metal−Organic Framework Membranes on Flexible Polymer Substrates. *Angew. Chem., Int. Ed.* **2016**, *55* (12), 3947−3951.
(50) Li, W.; Su, P.; Li, Z.; Xu, Z.; Wang, F.; Ou, H.; Zhang, J.; Zhang, G.; Zeng, E. Ultrathin Metal−organic Framework Membrane Production by Gel−vapour Deposition. *Nat. Commun.* **2017**, *8* (1), 406.
(51) He, G.; Dakhchoune, M.; Zhao, J.; Huang, S.; Agrawal, K. V. Electrophoretic Nuclei Assembly for Crystallization of High-Performance Membranes on Unmodified Supports. *Adv. Funct. Mater.* **2018**, *28* (20), 1707427.
(52) He, G.; Babu, D. J.; Agrawal, K. V. Electrophoretic Crystallization of Ultrathin High-Performance Metal-Organic Framework Membranes. *J. Visualized Exp.* **2018**, *138*, e58301.
(53) Ranjan, R.; Tsapatsis, M. Microporous Metal Organic Framework Membrane on Porous Support Using the Seeded Growth Method. *Chem. Mater.* **2009**, *21* (20), 4920−4924.
(54) Ge, L.; Zhou, W.; Du, A.; Zhu, Z. Porous Polyethersulfone-Supported Zeolitic Imidazolate Framework Membranes for Hydrogen Separation. *J. Phys. Chem. C* **2012**, *116* (24), 13264−13270.
(55) Venna, S. R.; Carreon, M. A. Highly Permeable Zeolite Imidazolate Framework-8 Membranes for CO2/CH4 Separation. *J. Am. Chem. Soc.* **2010**, *132* (1), 76−78.
(56) Li, Y.-S. S.; Liang, F.-Y. Y.; Bux, H.; Feldhoff, A.; Yang, W.-S. S.; Caro, J. Molecular Sieve Membrane: Supported Metal−organic Framework with High Hydrogen Selectivity. *Angew. Chem.* **2010**, *122* (3), 558−561.
(57) Zhong, Z.; Yao, J.; Chen, R.; Low, Z.; He, M.; Liu, J. Z.; Wang, H. Oriented Two-Dimensional Zeolitic Imidazolate Framework-L Membranes and Their Gas Permeation Properties. *J. Mater. Chem. A* **2015**, *3* (30), 15715−15722.
(58) Li, Y.; Liang, F.; Bux, H.; Yang, W.; Caro, J. Zeolitic Imidazolate Framework ZIF-7 Based Molecular Sieve Membrane for Hydrogen Separation. *J. Membr. Sci.* **2010**, *354* (1−2), 48−54.
(59) Bux, H.; Feldhoff, A.; Cravillon, J.; Wiebcke, M.; Li, Y.-S. S.; Caro, J. Oriented Zeolitic Imidazolate Framework-8 Membrane with Sharp H2/C3H8Molecular Sieve Separation. *Chem. Mater.* **2011**, *23* (8), 2262−2269.
(60) Li, Y.-S.; Bux, H.; Feldhoff, A.; Li, G.-L.; Yang, W.-S.; Caro, J. Controllable Synthesis of Metal-Organic Frameworks: From MOF Nanorods to Oriented MOF Membranes. *Adv. Mater.* **2010**, *22* (30), 3322−3326.
(61) Liu, Q.; Wang, N.; Caro, J.; Huang, A. Bio-Inspired Polydopamine: A Versatile and Powerful Platform for Covalent Synthesis of Molecular Sieve Membranes. *J. Am. Chem. Soc.* **2013**, *135* (47), 17679−17682.
(62) Shamsaei, E.; Lin, X.; Wan, L.; Tong, Y.; Wang, H. A One-Dimensional Material as a Nano-Scaffold and a Pseudo-Seed for Facilitated Growth of Ultrathin, Mechanically Reinforced Molecular Sieving Membranes. *Chem. Commun.* **2016**, *52* (95), 13764−13767.
(63) Wang, N.; Liu, Y.; Qiao, Z.; Diestel, L.; Zhou, J.; Huang, A.; Caro, J. Polydopamine-Based Synthesis of a Zeolite Imidazolate Framework ZIF-100 Membrane with High H2/CO2 Selectivity. *J. Mater. Chem. A* **2015**, *3* (8), 4722−4728.
(64) Zhang, S.; Wang, Z.; Ren, H.; Zhang, F.; Jin, J. Nanoporous Film-Mediated Growth of Ultrathin and Continuous Metal−organic Framework Membranes for High-Performance Hydrogen Separation. *J. Mater. Chem. A* **2017**, *5* (5), 1962−1966.
(65) Yang, H.-C.; Waldman, R. Z.; Wu, M.-B.; Hou, J.; Chen, L.; Darling, S. B.; Xu, Z.-K. Dopamine: Just the Right Medicine for Membranes. *Adv. Funct. Mater.* **2018**, *28* (8), 1705327.
(66) Huang, A.; Bux, H.; Steinbach, F.; Caro, J. Molecular-Sieve Membrane with Hydrogen Permselectivity: ZIF-22 in LTA Topology Prepared with 3-Aminopropyltriethoxysilane as Covalent Linker. *Angew. Chem., Int. Ed.* **2010**, *49* (29), 4958−4961.
(67) Huang, A.; Dou, W.; Caro, J. Steam-Stable Zeolitic Imidazolate Framework ZIF-90 Membrane with Hydrogen Selectivity through Covalent Functionalization. *J. Am. Chem. Soc.* **2010**, *132* (44), 15562−15564.
(68) Guerrero, V. V.; Yoo, Y.; McCarthy, M. C.; Jeong, H.-K. HKUST-1 Membranes on Porous Supports Using Secondary Growth. *J. Mater. Chem.* **2010**, *20* (19), 3938−3943.
(69) McCarthy, M. C.; Varela-Guerrero, V.; Barnett, G. V.; Jeong, H.-K. Synthesis of Zeolitic Imidazolate Framework Films and Membranes with Controlled Microstructures. *Langmuir* **2010**, *26* (18), 14636−14641.
(70) Kwon, H. T.; Jeong, H.-K. Highly Propylene-Selective Supported Zeolite-Imidazolate Framework (ZIF-8) Membranes Synthesized by Rapid Microwave-Assisted Seeding and Secondary Growth. *Chem. Commun.* **2013**, *49* (37), 3854−3856.
(71) Hillman, F.; Brito, J.; Jeong, H.-K. K. Rapid One-Pot Microwave Synthesis of Mixed-Linker Hybrid Zeolitic-Imidazolate Framework Membranes for Tunable Gas Separations. *ACS Appl. Mater. Interfaces* **2018**, *10* (6), 5586−5593.
(72) Hillman, F.; Zimmerman, J. M.; Paek, S.-M.; Hamid, M. R. A.; Lim, W. T.; Jeong, H.-K. Rapid Microwave-Assisted Synthesis of Hybrid Zeolitic−imidazolate Frameworks with Mixed Metals and Mixed Linkers. *J. Mater. Chem. A* **2017**, *5* (13), 6090−6099.
(73) Pan, Y.; Li, T.; Lestari, G.; Lai, Z. Effective Separation of Propylene/propane Binary Mixtures by ZIF-8 Membranes. *J. Membr. Sci.* **2012**, *390*, 93−98.
(74) Wang, X.-G.; Cheng, Q.; Yu, Y.; Zhang, X.-Z. Controlled Nucleation and Controlled Growth for Size Predicable Synthesis of Nanoscale Metal−Organic Frameworks (MOFs): A General and

DOI: 10.1021/acssuschemeng.8b05409
ACS Sustainable Chem. Eng. 2019, 7, 49−69

Scalable Approach. *Angew. Chem., Int. Ed.* **2018**, *57* (26), 7836−7840.
(75) Cacho-Bailo, F.; Catalán-Aguirre, S.; Etxeberría-Benavides, M.; Karvan, O.; Sebastian, V.; Téllez, C.; Coronas, J. Metal-Organic Framework Membranes on the Inner-Side of a Polymeric Hollow Fiber by Microfluidic Synthesis. *J. Membr. Sci.* **2015**, *476*, 277−285.
(76) Xie, Z.; Yang, J.; Wang, J.; Bai, J.; Yin, H.; Yuan, B.; Lu, J.; Zhang, Y.; Zhou, L.; Duan, C. Deposition of Chemically Modified α-Al2O3particles for High Performance ZIF-8 Membrane on a Macroporous Tube. *Chem. Commun.* **2012**, *48* (48), 5977−5979.
(77) Li, W.; Meng, Q.; Zhang, C.; Zhang, G. Metal−Organic Framework/PVDF Composite Membranes with High H2 Permselectivity Synthesized by Ammoniation. *Chem. - Eur. J.* **2015**, *21* (19), 7224−7230.
(78) Shamsaei, E.; Low, Z.-X.; Lin, X.; Mayahi, A.; Liu, H.; Zhang, X.; Zhe Liu, J.; Wang, H. Rapid Synthesis of Ultrathin, Defect-Free ZIF-8 Membranes via Chemical Vapour Modification of a Polymeric Support. *Chem. Commun.* **2015**, *51* (57), 11474−11477.
(79) Pan, Y.; Wang, B.; Lai, Z. Synthesis of Ceramic Hollow Fiber Supported Zeolitic Imidazolate Framework-8 (ZIF-8) Membranes with High Hydrogen Permeability. *J. Membr. Sci.* **2012**, *421*, 292−298.
(80) Xu, G.; Yao, J.; Wang, K.; He, L.; Webley, P. A.; Chen, C.; Wang, H. Preparation of ZIF-8 Membranes Supported on Ceramic Hollow Fibers from a Concentrated Synthesis Gel. *J. Membr. Sci.* **2011**, *385*, 187−193.
(81) Liu, D.; Ma, X.; Xi, H.; Lin, Y. S. S. Gas Transport Properties and Propylene/propane Separation Characteristics of ZIF-8 Membranes. *J. Membr. Sci.* **2014**, *451*, 85−93.
(82) Huang, K.; Dong, Z.; Li, Q.; Jin, W. Growth of a ZIF-8 Membrane on the Inner-Surface of a Ceramic Hollow Fiber via Cycling Precursors. *Chem. Commun.* **2013**, *49* (87), 10326−10328.
(83) Zhang, X.; Liu, Y.; Kong, L.; Liu, H.; Qiu, J.; Han, W.; Weng, L.-T.; Yeung, K. L.; Zhu, W. A Simple and Scalable Method for Preparing Low-Defect ZIF-8 Tubular Membranes. *J. Mater. Chem. A* **2013**, *1* (36), 10635−10638.
(84) Cacho-Bailo, F.; Seoane, B.; Téllez, C.; Coronas, J. ZIF-8 Continuous Membrane on Porous Polysulfone for Hydrogen Separation. *J. Membr. Sci.* **2014**, *464*, 119−126.
(85) Liu, Y.; Wang, N.; Pan, J. H.; Steinbach, F.; Caro, J. In Situ Synthesis of MOF Membranes on ZnAl-CO3 LDH Buffer Layer-Modified Substrates. *J. Am. Chem. Soc.* **2014**, *136* (41), 14353−14356.
(86) Su, P.; Li, W.; Zhang, C.; Meng, Q.; Shen, C.; Zhang, G. Metal Based Gels as Versatile Precursors to Synthesize Stiff and Integrated MOF/polymer Composite Membranes. *J. Mater. Chem. A* **2015**, *3* (40), 20345−20351.
(87) Liu, Y.; Pan, J. H.; Wang, N.; Steinbach, F.; Liu, X.; Caro, J.; et al. Remarkably Enhanced Gas Separation by Partial Self-Conversion of a Laminated Membrane to Metal−Organic Frameworks. *Angew. Chem.* **2015**, *127* (10), 3071−3075.
(88) Cacho-Bailo, F.; Caro, G.; Etxeberría-Benavides, M.; Karvan, O.; Téllez, C.; Coronas, J. MOF−polymer Enhanced Compatibility: Post-Annealed Zeolite Imidazolate Framework Membranes inside Polyimide Hollow Fibers. *RSC Adv.* **2016**, *6* (7), 5881−5889.
(89) Shekhah, O.; Swaidan, R.; Belmabkhout, Y.; du Plessis, M.; Jacobs, T.; Barbour, L. J.; Pinnau, I.; Eddaoudi, M. The Liquid Phase Epitaxy Approach for the Successful Construction of Ultra-Thin and Defect-Free ZIF-8 Membranes: Pure and Mixed Gas Transport Study. *Chem. Commun.* **2014**, *50* (17), 2089.
(90) Li, W.; Wu, W.; Li, Z.; Shi, J.; Xia, Y. Sol−gel Asynchronous Crystallization of Ultra-Selective Metal−organic Framework Membranes for Gas Separation. *J. Mater. Chem. A* **2018**, *6* (34), 16333−16340.
(91) Zhu, Y.; Ciston, J.; Zheng, B.; Miao, X.; Czarnik, C.; Pan, Y.; Sougrat, R.; Lai, Z.; Hsiung, C.-E. E.; Yao, K.; et al. Unravelling Surface and Interfacial Structures of a Metal-Organic Framework by Transmission Electron Microscopy. *Nat. Mater.* **2017**, *16* (5), 532−536.
(92) Newsome, D. A.; Sholl, D. S. Molecular Dynamics Simulations of Mass Transfer Resistance in Grain Boundaries of Twinned Zeolite Membranes. *J. Phys. Chem. B* **2006**, *110* (45), 22681−22689.
(93) Choi, J.; Jeong, H.-K. H.-K.; Snyder, M. A. M. A.; Stoeger, J. A. J. A.; Masel, R. I. R. I.; Tsapatsis, M. Grain Boundary Defect Elimination in a Zeolite Membrane by Rapid Thermal Processing. *Science* **2009**, *325* (5940), 590−593.
(94) Liu, J.; Wöll, C. Surface-Supported Metal−organic Framework Thin Films: Fabrication Methods, Applications, and Challenges. *Chem. Soc. Rev.* **2017**, *46* (19), 5730−5770.
(95) Liu, Y.; Ban, Y.; Yang, W. Microstructural Engineering and Architectural Design of Metal−Organic Framework Membranes. *Adv. Mater.* **2017**, *29* (31), 1−17.
(96) Sun, Y.; Yang, F.; Wei, Q.; Wang, N.; Qin, X.; Zhang, S.; Wang, B.; Nie, Z.; Ji, S.; Yan, H.; et al. Oriented Nano-Microstructure-Assisted Controllable Fabrication of Metal-Organic Framework Membranes on Nickel Foam. *Adv. Mater.* **2016**, *28* (12), 2374−2381.
(97) Sun, Y.; Liu, Y.; Caro, J.; Guo, X.; Song, C.; Liu, Y. In-Plane Epitaxial Growth of Highly c-Oriented NH2-MIL-125(Ti) Membranes with Superior H2/CO2 Selectivity. *Angew. Chem., Int. Ed.* **2018**, *57* (49), 16088−16093.
(98) Friebe, S.; Mundstock, A.; Unruh, D.; Renz, F.; Caro, J. NH2-MIL-125 as Membrane for Carbon Dioxide Sequestration: Thin Supported MOF Layers Contra Mixed-Matrix-Membranes. *J. Membr. Sci.* **2016**, *516*, 185−193.
(99) Gücüyener, C.; van den Bergh, J.; Gascon, J.; Kapteijn, F. Ethane/Ethene Separation Turned on Its Head: Selective Ethane Adsorption on the Metal−Organic Framework ZIF-7 through a Gate-Opening Mechanism. *J. Am. Chem. Soc.* **2010**, *132* (50), 17704−17706.
(100) Aguado, S.; Bergeret, G.; Titus, M. P.; Moizan, V.; Nieto-Draghi, C.; Bats, N.; Farrusseng, D. Guest-Induced Gate-Opening of a Zeolite Imidazolate Framework. *New J. Chem.* **2011**, *35* (3), 546−550.
(101) Zhang, C.; Lively, R. P.; Zhang, K.; Johnson, J. R.; Karvan, O.; Koros, W. J. Unexpected Molecular Sieving Properties of Zeolitic Imidazolate Framework-8. *J. Phys. Chem. Lett.* **2012**, *3* (16), 2130−2134.
(102) Chokbunpiam, T.; Fritzsche, S.; Caro, J.; Chmelik, C.; Janke, W.; Hannongbua, S. Importance of ZIF-90 Lattice Flexibility on Diffusion, Permeation, and Lattice Structure for an Adsorbed H2/CH4 Gas Mixture: A Re-Examination by Gibbs Ensemble Monte Carlo and Molecular Dynamics Simulations. *J. Phys. Chem. C* **2017**, *121* (19), 10455−10462.
(103) Bourrelly, S.; Llewellyn, P. L.; Serre, C.; Millange, F.; Loiseau, T.; Férey, G. Different Adsorption Behaviors of Methane and Carbon Dioxide in the Isotypic Nanoporous Metal Terephthalates MIL-53 and MIL-47. *J. Am. Chem. Soc.* **2005**, *127* (39), 13519−13521.
(104) Moggach, S. A.; Bennett, T. D.; Cheetham, A. K. The Effect of Pressure on ZIF-8: Increasing Pore Size with Pressure and the Formation of a High-Pressure Phase at 1.47 GPa. *Angew. Chem., Int. Ed.* **2009***48* (38), 7087−7089.
(105) Fairen-Jimenez, D.; Moggach, S. A.; Wharmby, M. T.; Wright, P. A.; Parsons, S.; Düren, T. Opening the Gate: Framework Flexibility in ZIF-8 Explored by Experiments and Simulations. *J. Am. Chem. Soc.* **2011**, *133* (23), 8900−8902.
(106) Kolokolov, D. I.; Stepanov, A. G.; Jobic, H. Mobility of the 2-Methylimidazolate Linkers in ZIF-8 Probed by 2H NMR: Saloon Doors for the Guests. *J. Phys. Chem. C* **2015**, *119* (49), 27512−27520.
(107) Casco, M. E.; Cheng, Y. Q.; Daemen, L. L.; Fairen-Jimenez, D.; Ramos-Fernández, E. V.; Ramirez-Cuesta, A. J.; Silvestre-Albero, J. Gate-Opening Effect in ZIF-8: The First Experimental Proof Using Inelastic Neutron Scattering. *Chem. Commun.* **2016**, *52* (18), 3639−3642.
(108) Casco, M. E.; Fernández-Catalá, J.; Cheng, Y.; Daemen, L.; Ramirez-Cuesta, A. J.; Cuadrado-Collados, C.; Silvestre-Albero, J.; Ramos-Fernandez, E. V. Understanding ZIF-8 Performance upon Gas

DOI: 10.1021/acssuschemeng.8b05409
ACS Sustainable Chem. Eng. 2019, 7, 49−69

Adsorption by Means of Inelastic Neutron Scattering. *ChemistrySelect* **2017**, *2* (9), 2750−2753.
(109) Huang, A.; Wang, N.; Kong, C.; Caro, J. Organosilica-Functionalized Zeolitic Imidazolate Framework ZIF-90 Membrane with High Gas-Separation Performance. *Angew. Chem., Int. Ed.* **2012**, *51* (42), 10551−10555.
(110) Thompson, J. A.; Blad, C. R.; Brunelli, N. A.; Lydon, M. E.; Lively, R. P.; Jones, C. W.; Nair, S. Hybrid Zeolitic Imidazolate Frameworks: Controlling Framework Porosity and Functionality by Mixed-Linker Synthesis. *Chem. Mater.* **2012**, *24* (10), 1930−1936.
(111) Kwon, H. T.; Jeong, H.-K. K.; Lee, A. S.; An, H. S.; Lee, J. S. Heteroepitaxially Grown Zeolitic Imidazolate Framework Membranes with Unprecedented Propylene/Propane Separation Performances. *J. Am. Chem. Soc.* **2015**, *137* (38), 12304−12311.
(112) Knebel, A.; Geppert, B.; Volgmann, K.; Kolokolov, D. I.; Stepanov, A. G.; Twiefel, J.; Heitjans, P.; Volkmer, D.; Caro, J. Defibrillation of Soft Porous Metal-Organic Frameworks with Electric Fields. *Science* **2017**, *358* (6361), 347−351.
(113) Zhou, S.; Wei, Y.; Li, L.; Duan, Y.; Hou, Q.; Zhang, L.; Ding, L.-X.; Xue, J.; Wang, H.; Caro, J. Paralyzed Membrane: Current-Driven Synthesis of a Metal-Organic Framework with Sharpened Propene/propane Separation. *Sci. Adv.* **2018**, *4* (10), eaau1393.
(114) Huang, A.; Liu, Q.; Wang, N.; Zhu, Y.; Caro, J. Bicontinuous Zeolitic Imidazolate Framework ZIF-8@GO Membrane with Enhanced Hydrogen Selectivity. *J. Am. Chem. Soc.* **2014**, *136* (42), 14686−14689.
(115) Li, C.-P.; Du, M. Role of Solvents in Coordination Supramolecular Systems. *Chem. Commun.* **2011**, *47* (21), 5958−5972.
(116) Zhao, P.; Lampronti, G. I.; Lloyd, G. O.; Wharmby, M. T.; Facq, S.; Cheetham, A. K.; Redfern, S. A. T. Phase Transitions in Zeolitic Imidazolate Framework 7: The Importance of Framework Flexibility and Guest-Induced Instability Scheme 1. Phase Transitions in ZIF-7. *Chem. Mater.* **2014**, *26*, 1767−1769.
(117) Sholl, D. S.; Lively, R. P. Defects in Metal−Organic Frameworks: Challenge or Opportunity? *J. Phys. Chem. Lett.* **2015**, *6* (17), 3437−3444.
(118) Fang, F.; Bueken, B.; De Vos, D. E.; Fischer, R. A. Defect-Engineered Metal−Organic Frameworks. *Angew. Chem., Int. Ed.* **2015**, *54* (25), 7234−7254.
(119) Bennett, T. D.; Cheetham, A. K.; Fuchs, A. H.; Coudert, F.-X. Interplay between Defects, Disorder and Flexibility in Metal-Organic Frameworks. *Nat. Chem.* **2016**, *9*, 11.
(120) Dissegna, S.; Epp, K.; Heinz, W. R.; Kieslich, G.; Fischer, R. A. Defective Metal-Organic Frameworks. *Adv. Mater.* **2018**, *30* (37), 1704501.
(121) Ameloot, R.; Vermoortele, F.; Hofkens, J.; De Schryver, F. C.; De Vos, D. E.; Roeffaers, M. B. J. Three-Dimensional Visualization of Defects Formed during the Synthesis of Metal−Organic Frameworks: A Fluorescence Microscopy Study. *Angew. Chem., Int. Ed.* **2013**, *52* (1), 401−405.
(122) Lee, M. J.; Kwon, H. T.; Jeong, H.-K. Defect-Dependent Stability of Highly Propylene-Selective Zeolitic-Imidazolate Framework ZIF-8 Membranes. *J. Membr. Sci.* **2017**, *529*, 105−113.
(123) Ravon, U.; Savonnet, M.; Aguado, S.; Domine, M. E.; Janneau, E.; Farrusseng, D. Engineering of Coordination Polymers for Shape Selective Alkylation of Large Aromatics and the Role of Defects. *Microporous Mesoporous Mater.* **2010**, *129* (3), 319−329.
(124) Bhattacharyya, S.; Pang, S. H.; Dutzer, M. R.; Lively, R. P.; Walton, K. S.; Sholl, D. S.; Nair, S. Interactions of SO2-Containing Acid Gases with ZIF-8: Structural Changes and Mechanistic Investigations. *J. Phys. Chem. C* **2016**, *120* (48), 27221−27229.
(125) Jayachandrababu, K. C.; Bhattacharyya, S.; Chiang, Y.; Sholl, D. S.; Nair, S. Recovery of Acid-Gas-Degraded Zeolitic Imidazolate Frameworks by Solvent-Assisted Crystal Redemption (SACRed). *ACS Appl. Mater. Interfaces* **2017**, *9* (40), 34597−34602.
(126) Kwon, H. T.; Jeong, H.-K.; Lee, A. S.; An, H. S.; Lee, T.; Jang, E.; Lee, J. S.; Choi, J. Defect-Induced Ripening of Zeolitic-Imidazolate Framework ZIF-8 and Its Implication to Vapor-Phase Membrane Synthesis. *Chem. Commun.* **2016**, *52* (78), 11669−11672.
(127) Eum, K.; Jayachandrababu, K. C.; Rashidi, F.; Zhang, K.; Leisen, J.; Graham, S.; Lively, R. P.; Chance, R. R.; Sholl, D. S.; Jones, C. W.; et al. Highly Tunable Molecular Sieving and Adsorption Properties of Mixed-Linker Zeolitic Imidazolate Frameworks. *J. Am. Chem. Soc.* **2015**, *137* (12), 4191−4197.
(128) Rashidi, F.; Blad, C. R.; Jones, C. W.; Nair, S. Synthesis, Characterization, and Tunable Adsorption and Diffusion Properties of Hybrid ZIF-7−90 Frameworks. *AIChE J.* **2016**, *62* (2), 525−537.
(129) Karagiaridi, O.; Bury, W.; Mondloch, J. E.; Hupp, J. T.; Farha, O. K. Solvent-Assisted Linker Exchange: An Alternative to the De Novo Synthesis of Unattainable Metal−Organic Frameworks. *Angew. Chem., Int. Ed.* **2014**, *53* (18), 4530−4540.
(130) Karagiaridi, O.; Lalonde, M. B.; Bury, W.; Sarjeant, A. A.; Farha, O. K.; Hupp, J. T. Opening ZIF-8: A Catalytically Active Zeolitic Imidazolate Framework of Sodalite Topology with Unsubstituted Linkers. *J. Am. Chem. Soc.* **2012**, *134* (45), 18790−18796.
(131) Jayachandrababu, K. C.; Sholl, D. S.; Nair, S. Structural and Mechanistic Differences in Mixed-Linker Zeolitic Imidazolate Framework Synthesis by Solvent Assisted Linker Exchange and de Novo Routes. *J. Am. Chem. Soc.* **2017**, *139* (16), 5906−5915.
(132) Lee, M. J.; Kwon, H. T.; Jeong, H.-K. K. *Angew. Chem., Int. Ed.* **2018**, *57* (1), 156−161.
(133) Li, W.; Zhang, Y.; Zhang, C.; Meng, Q.; Xu, Z.; Su, P.; Li, Q.; Shen, C.; Fan, Z.; Qin, L.; et al. Transformation of Metal-Organic Frameworks for Molecular Sieving Membranes. *Nat. Commun.* **2016**, *7*, 11315.
(134) Kwon, H. T.; Jeong, H.-K. In Situ Synthesis of Thin Zeolitic−imidazolate Framework ZIF-8 Membranes Exhibiting Exceptionally High Propylene/propane Separation. *J. Am. Chem. Soc.* **2013**, *135* (29), 10763−10768.
(135) Zhang, H.; Hou, J.; Hu, Y.; Wang, P.; Ou, R.; Jiang, L.; Liu, J. Z.; Freeman, B. D.; Hill, A. J.; Wang, H. Ultrafast Selective Transport of Alkali Metal Ions in Metal Organic Frameworks with Subnanometer Pores. *Sci. Adv.* **2018**, *4* (2), eaaq0066.
(136) Liu, X.; Wang, C.; Wang, B.; Li, K. Novel Organic-Dehydration Membranes Prepared from Zirconium Metal-Organic Frameworks. *Adv. Funct. Mater.* **2017**, *27* (3), 1604311.
(137) Li, J.-R.; Sculley, J.; Zhou, H.-C. Metal−Organic Frameworks for Separations. *Chem. Rev.* **2012**, *112* (2), 869−932.
(138) Sheng, L.; Wang, C.; Yang, F.; Xiang, L.; Huang, X.; Yu, J.; Zhang, L.; Pan, Y.; Li, Y. Enhanced C3H6/C3H8 Separation Performance on MOF Membranes through Blocking Defects and Hindering Framework Flexibility by Silicone Rubber Coating. *Chem. Commun.* **2017**, *53* (55), 7760−7763.
(139) Burns, R. L.; Koros, W. J. Defining the Challenges for C3H6/C3H8 Separation Using Polymeric Membranes. *J. Membr. Sci.* **2003**, *211* (2), 299−309.
(140) Wang, C.; Yang, F.; Sheng, L.; Yu, J.; Yao, K.; Zhang, L.; Pan, Y. Zinc-Substituted ZIF-67 Nanocrystals and Polycrystalline Membranes for Propylene/propane Separation. *Chem. Commun.* **2016**, *52* (85), 12578−12581.
(141) Cacho-Bailo, F.; Etxeberría-Benavides, M.; David, O.; Téllez, C.; Coronas, J. Structural Contraction of Zeolitic Imidazolate Frameworks: Membrane Application on Porous Metallic Hollow Fibers for Gas Separation. *ACS Appl. Mater. Interfaces* **2017**, *9* (24), 20787−20796.
(142) Huang, A.; Chen, Y.; Wang, N.; Hu, Z.; Jiang, J.; Caro, J. A Highly Permeable and Selective Zeolitic Imidazolate Framework ZIF-95 Membrane for H2/CO2 Separation. *Chem. Commun.* **2012**, *48* (89), 10981−10983.
(143) Kang, Z.; Xue, M.; Fan, L.; Huang, L.; Guo, L.; Wei, G.; Chen, B.; Qiu, S. Highly Selective Sieving of Small Gas Molecules by Using an Ultra-Microporous Metal−organic Framework Membrane. *Energy Environ. Sci.* **2014**, *7* (12), 4053−4060.
(144) Zhang, F.; Zou, X. Q.; Gao, X.; Fan, S. J.; Sun, F. X.; Ren, H.; Zhu, G. S. Hydrogen Selective NH2-MIL-53(Al) MOF Membranes

DOI: 10.1021/acssuschemeng.8b05409
ACS Sustainable Chem. Eng. 2019, 7, 49−69

with High Permeability. *Adv. Funct. Mater.* **2012**, *22* (17), 3583−3590.
(145) Merkel, T. C.; Zhou, M.; Baker, R. W. Carbon Dioxide Capture with Membranes at an IGCC Power Plant. *J. Membr. Sci.* **2012**, *389*, 441−450.
(146) Huang, A.; Liu, Q.; Wang, N.; Caro, J. Highly Hydrogen Permselective ZIF-8 Membranes Supported on Polydopamine Functionalized Macroporous Stainless-Steel-Nets. *J. Mater. Chem. A* **2014**, *2* (22), 8246−8251.
(147) Melgar, V. M. A.; Kwon, H. T.; Kim, J. Direct Spraying Approach for Synthesis of ZIF-7 Membranes by Electrospray Deposition. *J. Membr. Sci.* **2014**, *459*, 190−196.
(148) Li, W.; Meng, Q.; Li, X.; Zhang, C.; Fan, Z.; Zhang, G. Non-Activation ZnO Array as a Buffering Layer to Fabricate Strongly Adhesive Metal−organic framework/PVDF Hollow Fiber Membranes. *Chem. Commun.* **2014**, *50* (68), 9711−9713.
(149) Kang, Z.; Wang, S.; Wang, R.; Guo, H.; Xu, B.; Feng, S.; Fan, L.; Zhu, L.; Kang, W.; Pang, J.; et al. Sandwich Membranes through a Two-Dimensional Confinement Strategy for Gas Separation. *Mater. Chem. Front.* **2018**, *2*, 1911−1919.
(150) Ben, T.; Lu, C.; Pei, C.; Xu, S.; Qiu, S. Polymer-Supported and Free-Standing Metal−Organic Framework Membrane. *Chem. - Eur. J.* **2012**, *18* (33), 10250−10253.
(151) Lee, D.-J.; Li, Q.; Kim, H.; Lee, K. Preparation of Ni-MOF-74 Membrane for CO2 Separation by Layer-by-Layer Seeding Technique. *Microporous Mesoporous Mater.* **2012**, *163*, 169−177.
(152) Huang, A.; Caro, J. Covalent Post-functionalization of Zeolitic Imidazolate Framework ZIF-90 Membrane for Enhanced Hydrogen Selectivity. *Angew. Chem., Int. Ed.* **2011**, *50* (21), 4979−4982.
(153) Wang, N.; Mundstock, A.; Liu, Y.; Huang, A.; Caro, J. Amine-Modified Mg-MOF-74/CPO-27-Mg Membrane with Enhanced H2/CO2 Separation. *Chem. Eng. Sci.* **2015**, *124*, 27−36.
(154) Guo, H.; Zhu, G.; Hewitt, I. J.; Qiu, S. Twin Copper Source" Growth of Metal− Organic Framework Membrane: Cu3(BTC)2 with High Permeability and Selectivity for Recycling H2. *J. Am. Chem. Soc.* **2009**, *131* (5), 1646−1647.
(155) Merkel, T. C.; Lin, H.; Wei, X.; Baker, R. Power Plant Post-Combustion Carbon Dioxide Capture: An Opportunity for Membranes. *J. Membr. Sci.* **2010**, *359* (1−2), 126−139.
(156) Yin, H.; Wang, J.; Xie, Z.; Yang, J.; Bai, J.; Lu, J.; Zhang, Y.; Yin, D.; Lin, J. Y. S. A Highly Permeable and Selective Amino-Functionalized MOF CAU-1 Membrane for CO2-N2separation. *Chem. Commun.* **2014**, *50* (28), 3699−3701.
(157) Jian, Y.; Yin, H.; Chang, F.; Cheng, L.; Yang, J.; Mu, W.; Li, X.; Lu, J.; Zhang, Y.; Wang, J. Facile Synthesis of Highly Permeable CAU-1 Tubular Membranes for Separation of CO2/N2Mixtures. *J. Membr. Sci.* **2017**, *522*, 140−150.
(158) Rui, Z.; James, J. B.; Kasik, A.; Lin, Y. S. Metal-organic Framework Membrane Process for High Purity CO2 Production. *AIChE J.* **2016**, *62* (11), 3836−3841.
(159) Kasik, A.; Lin, Y. S. Organic Solvent Pervaporation Properties of MOF-5 Membranes. *Sep. Purif. Technol.* **2014**, *121*, 38−45.
(160) Peng, Y.; Li, Y.; Ban, Y.; Jin, H.; Jiao, W.; Liu, X.; Yang, W. Metal-Organic Framework Nanosheets as Building Blocks for Molecular Sieving Membranes. *Science* **2014**, *346* (6215), 1356−1359.

DOI: 10.1021/acssuschemeng.8b05409
ACS Sustainable Chem. Eng. 2019, 7, 49−69